IEEE Access
Multidisciplinary | Rapid Review | Open Access Journal

Received July 12, 2019, accepted July 23, 2019, date of publication August 2, 2019, date of current version September 5, 2019.

Digital Object Identifier 10.1109/ACCESS.2019.2932748

Calibrating the Transmitter and Receiver Location Errors for Moving Target Localization in Multistatic Passive Radar

YONGSHENG ZHAO, DEXIU HU, ZHIXIN LIU, AND YONGJUN ZHAO
PLA Strategic Support Force Information Engineering University, Zhengzhou 450001, China

Corresponding author: Dexiu Hu (paper_hdx@126.com)

This work was supported in part by the National Natural Science Foundation of China under Grant 61703433.

ABSTRACT The presence of transmitter and receiver location uncertainties has been known to remarkably deteriorate the target localization accuracy in multi-static passive radar (MPR) system. This paper explores the use of calibration targets, the positions and velocities of which are known to the MPR system, to counter the loss in target localization accuracy arising from the transmitter/receiver location uncertainties. We firstly evaluate the Cramér-Rao lower bound (CRLB) for bistatic range (BR) and bistatic range rate (BRR)-based target localization in the presence of calibration targets, which analytically indicates the potential of calibration targets in enhancing localization accuracy. After that, a novel closed-form solution is proposed for target localization using the BR and BRR measurements from the unknown target as well as the additional BR and BRR measurements from the calibration targets. The proposed solution includes two processing steps, referred to as calibration step and localization step respectively. The calibration step is devoted to refine the inaccurate transmitter and receiver locations using the BR and BRR measurements from the calibration targets, and then the localization step is devoted to determine the target position and velocity based on the refined transmitter/receiver locations and the BR/BRR measurements from the unknown target. The accuracy of proposed solution is shown analytically to accomplish the CRLB under sufficiently small BR/BRR measurement noises and transmitter/receiver location errors. Simulation results verify the effectiveness and superiority of the proposed solution over existing algorithms.

INDEX TERMS Calibration target, transmitter and receiver location uncertainty, multistatic passive radar, bistatic range, bistatic range rate, Cramér-Rao lower bound.

I. INTRODUCTION

With no dedicated transmitter, passive radar detects and tracks potential targets by processing reflections from non-cooperative transmitters in the environment, such as commercial broadcast/communication transmission [1] and non-cooperative radar emitters [2]. This special working principle gives passive radar many obvious advantages including lower-cost, lower-power, and more covert surveillance capability compared to active radar technology [3]. In the last decade, passive radar technology has received continuously growing attention from the research community due to its potential applications in homeland security, coastal surveillance, early warning system for vehicle detection, and so on.

The associate editor coordinating the review of this article and approving it for publication was Jaime Lloret.

A passive radar receiver generally employs two receiving channels, termed as reference channel and surveillance channel respectively. The reference channel is used to sense the direct path signal from the transmitter, and the surveillance channel is used to capture the potential target echoes [4]. Subsequently, by performing the delay-Doppler cross-correlation between the direct path signal and the target echo signal, the time delay (TD) and Doppler shift (DS) can be measured [5], which hold information on the target position and velocity. By combining the passive radar geometry configuration, the TD can be directly translated into the bistatic range (BR) which is defined as the sum of transmitter-target and target-receiver ranges [6], and the DS can be translated into the bistatic range rate (BRR). For multistatic passive radar (MPR), if enough BR and BRR measurements corresponding to the multiple transmitter-receiver pairs are

available, the target position and velocity can be estimated by solving the set of nonlinear BR and BRR measurement equations. Nevertheless, due to the nonlinear relationships between the BR/BRR measurements and the desired target location parameters, BR-and-BRR-based target localization problem is potentially challenging.

In recent years, several efficient algorithms have been proposed for this challenging problem. Taking inspiration from the well-known two-step weighted least squares (2WLS) idea of Ho and Xu [7], Du and Wei [8] explored an efficient closed-form solution for the estimation of the target position and velocity in a noncoherent distributed MIMO radar using the BR and BRR measurements. By dividing these measurements into several groups according to different transmitters or receivers and then applying two-step weighted least squares minimization on each group, several independent estimates of target position and velocity are produced, which are subsequently merged to form the final estimate. However, this method could only obtain a suboptimal estimate of target position and velocity if the measurement noises from different groups are correlated. To this end, Yang and Chun [9] introduced an improved 2WLS framework without grouping and merging for moving target localization in noncoherent MIMO radar systems. It requires one transmitter or receiver as the reference, and translates the BR and BRR measurements into the RD and RRD ones. However, this method suffers from a loss in the localization accuracy, since translating the BR and BRR measurements into the RD and RRD ones results in a loss of measurement equations. By introducing multiple auxiliary variables, Zhao *et al.* develop a novel algebraic solution for target position and velocity estimation in [10], where the first WLS step linearizes the BR and BRR measurement equations by introducing multiple auxiliary variables and produces a rough estimate using WLS minimization, then the second step explores the relation between the auxiliary variables and the target location parameters to refine the estimate. This method requires neither grouping and merging nor translating the BR and BRR measurements into the RD and RRD ones, and is proven analytically and numerically to reach the Cramér-Rao lower bound (CRLB) accuracy.

Nevertheless, the above studies are based on the assumption that the transmitter and receiver location parameters are known perfectly, which is not realistic. In practice, the transmitter and receiver location parameters, in both positions and velocities, will inevitably have errors, which are also known as location uncertainties. The transmitter and receiver location errors often cannot be ignored, when for example the transmitters and/or receivers are mounted on the moving platforms [11], [12], again for example the employed transmitters are highly non-cooperative hostile radar radiation whose location parameters could only be roughly measured by electronic support measures (ESM) receivers [13], [14]. The recent work of Zhao *et al.* [15] explored the effect of the transmitter and receiver location errors on the target localization accuracy at the CRLB level, and then design a solution that takes the transmitter and receiver location error into account to reduce the target localization error. By using the statistical distributions of the transmitter and receiver location errors, this method is shown analytically and numerically to accomplish the CRLB accuracy under some mild approximations. Nevertheless, this method does not fundamentally reduce the performance loss caused by the transmitter and receiver location error, that is, its localization accuracy is still substantially lower than that when the transmitter and receiver location errors are absent.

Calibration technique is not a new idea. It has been widely used in wireless sensor network self-localization [16], [17], where each sensor emits signals to and receives signals from other sensors, in order to estimate their locations collaboratively. Hasan explores in [18] a calibration algorithm to improve the direction finding performance using passive sensor arrays whose manifold is only nominally known. Ho and Yang [19], [20] apply the calibration technique to range difference (RD)-based source localization problem, where calibration sensors with known positions are deployed and additional RD measurements from the calibration sensors are incorporated to reduce the loss in localization accuracy caused by the sensor position uncertainties. Li *et al.* [21] further expand this idea to the RD and range difference rate (RRD)-based source localization problem. The successful application of calibration techniques in these areas suggests the possibility of employing the calibration technique in target localization for multi-static passive radar. When it comes to the target localization in multi-static passive radar, using 'calibration targets' with known locations may also be able to mitigate the target localization performance loss resulting from the transmitter/receiver location uncertainties. In theory, any target appearing in the radar coverage area and meanwhile broadcasting its locations, can be used as a calibration target. Typically, for example, to avoid potential accidents and collisions, the commercial aircrafts will report their locations and other information to the ground stations and other aircrafts, through the Automatic Dependent Surveillance Broadcast (ADS-B) system [22]. Hence, these commercial aircrafts can be considered as off-the-shelf calibration targets. If no such off-the-shelf calibration targets are available in the radar coverage area, we can manually launch some aircrafts with known locations as calibration targets. However, despite the fine prospects, up to now there does not exist any publication in the open literature that addresses using calibration targets to refine the nominal transmitter and receiver locations and reduce the loss in target localization accuracy caused by the transmitter and receiver location uncertainties for multi-static passive radar.

Motivated by these facts, in this paper, taking the transmitter and receiver location uncertainties into consideration, we explore using calibration targets to counter the loss in BR-and-BRR-based target localization accuracy induced by the transmitter/receiver location uncertainties. We begin our work by deriving the CRLB for BR-and-BRR-based target localization when the BR and BRR measurements with

respect to the calibration targets are available. The interpretation on the CRLB demonstrates that the use of calibration targets can potentially reduce the influence of the transmitter/receiver location uncertainties and enhance the target localization accuracy at the CRLB level. We then proceed to develop a novel localization algorithm to refine the nominal transmitter and receiver localization locations and hence estimate the target locations with higher accuracy. It can be divided into two processing steps, referred to as calibration step and localization step respectively. In the calibration step, the BR and BRR measurements from the calibration targets are exploited to refine the nominal transmitter and receiver locations; in the localization step, the refined transmitter and receiver locations and the BR/BRR measurements from the unknown target are exploited to determine the target position and velocity. Both processing steps are closed-form, which brings the proposed solution computational efficiency and high robustness. Moreover, the accuracy of proposed solution is shown analytically to reach the CRLB under some mild conditions. Simulations will be conducted to verify the effectiveness and superiority of the proposed solution over existing algorithms.

Notations: Without exception, we shall use bold lower case letter to denote column vector and bold upper case letter to represent matrix. Also, notations $(\cdot)^{\mathrm{o}}$, $(\cdot)^{\mathrm{T}}$, $\|\cdot\|$, $(\cdot)^{-1}$, $\mathrm{E}(\cdot)$, $\mathbf{O}_{p\times q}$, $\mathbf{I}_p$, $\mathbf{0}_{p\times 1}$, $\mathrm{diag}(\cdot)$ and $\mathrm{tr}(\cdot)$, denote the true value of a noisy or an estimated value, transpose operation, Euclidean norm, inverse of a matrix, statistical expectation, a p-by-q zero matrix, an p-by-p identity matrix, a p-by-1 zero vector, a diagonal matrix and the trace of a matrix, respectively.

The rest of the study is organized as follows. Section II describes the localization scenario in the presence of transmitter/receiver uncertainties and calibration targets. Section III characterizes the potential performance improvement from the use of calibration targets by evaluating the CRLB with calibration targets. Section IV is devoted to derive the proposed solution, and the theoretical performance analysis is also given in this section. Section V presents simulation results to evaluate the performance of the proposed solution and compares it with existing algorithms as well as the CRLB. Finally, Section VI concludes the paper.

II. LOCALIZATION SCENARIO

We shall address a localization scenario as shown in FIGURE 1, where a multistatic passive radar system with M transmitters and N receivers is deployed to determine the position $\mathbf{u}^{\mathrm{o}} = [x^{\mathrm{o}}, y^{\mathrm{o}}, z^{\mathrm{o}}]^{\mathrm{T}}$ and velocity $\dot{\mathbf{u}}^{\mathrm{o}} = [\dot{x}^{\mathrm{o}}, \dot{y}^{\mathrm{o}}, \dot{z}^{\mathrm{o}}]^{\mathrm{T}}$ of a single moving target using the BR and BRR measurements. The positions and velocities of the transmitters are denoted by $\mathbf{s}_{\mathrm{t}}^{\mathrm{o}} = [(\mathbf{s}_{\mathrm{t},1}^{\mathrm{o}})^{\mathrm{T}}, (\mathbf{s}_{\mathrm{t},2}^{\mathrm{o}})^{\mathrm{T}}, \ldots, (\mathbf{s}_{\mathrm{t},M}^{\mathrm{o}})^{\mathrm{T}}]^{\mathrm{T}}$ and $\dot{\mathbf{s}}_{\mathrm{t}}^{\mathrm{o}} = [(\dot{\mathbf{s}}_{\mathrm{t},1}^{\mathrm{o}})^{\mathrm{T}}, (\dot{\mathbf{s}}_{\mathrm{t},2}^{\mathrm{o}})^{\mathrm{T}}, \ldots, (\dot{\mathbf{s}}_{\mathrm{t},M}^{\mathrm{o}})^{\mathrm{T}}]^{\mathrm{T}}$, where $\mathbf{s}_{\mathrm{t},m}^{\mathrm{o}} = [x_{\mathrm{t},m}^{\mathrm{o}}, y_{\mathrm{t},m}^{\mathrm{o}}, z_{\mathrm{t},m}^{\mathrm{o}}]^{\mathrm{T}}$ and $\dot{\mathbf{s}}_{\mathrm{t},m}^{\mathrm{o}} = [\dot{x}_{\mathrm{t},m}^{\mathrm{o}}, \dot{y}_{\mathrm{t},m}^{\mathrm{o}}, \dot{z}_{\mathrm{t},m}^{\mathrm{o}}]^{\mathrm{T}}$ represent the position and velocity of transmitter m, $m = 1, 2, \ldots, M$; The positions and velocities of the receivers are denoted by $\mathbf{s}_{\mathrm{r}}^{\mathrm{o}} = [(\mathbf{s}_{\mathrm{r},1}^{\mathrm{o}})^{\mathrm{T}}, (\mathbf{s}_{\mathrm{r},2}^{\mathrm{o}})^{\mathrm{T}}, \ldots, (\mathbf{s}_{\mathrm{r},N}^{\mathrm{o}})^{\mathrm{T}}]^{\mathrm{T}}$ and $\dot{\mathbf{s}}_{\mathrm{r}}^{\mathrm{o}} = [(\dot{\mathbf{s}}_{\mathrm{r},1}^{\mathrm{o}})^{\mathrm{T}}, (\dot{\mathbf{s}}_{\mathrm{r},2}^{\mathrm{o}})^{\mathrm{T}}, \ldots, (\dot{\mathbf{s}}_{\mathrm{r},N}^{\mathrm{o}})^{\mathrm{T}}]^{\mathrm{T}}$, where $\mathbf{s}_{\mathrm{r},n}^{\mathrm{o}} = [x_{\mathrm{r},n}^{\mathrm{o}}, y_{\mathrm{r},n}^{\mathrm{o}}, z_{\mathrm{r},n}^{\mathrm{o}}]^{\mathrm{T}}$ and $\dot{\mathbf{s}}_{\mathrm{r},n}^{\mathrm{o}} = [\dot{x}_{\mathrm{r},n}^{\mathrm{o}}, \dot{y}_{\mathrm{r},n}^{\mathrm{o}}, \dot{z}_{\mathrm{r},n}^{\mathrm{o}}]^{\mathrm{T}}$ denote the position and velocity of receiver n, $n = 1, 2, \ldots, N$. In this work, the transmitter and receiver location parameters are not known perfectly and the available versions are

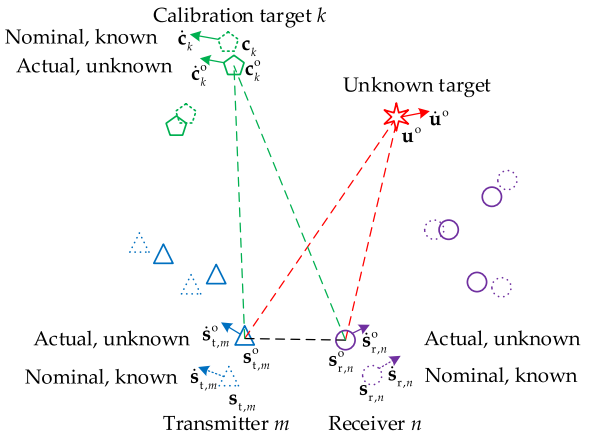

FIGURE 1. A typical localization scenario of multistatic passive radar.

$$\mathbf{s}_{\mathrm{t},m} = \mathbf{s}_{\mathrm{t},m}^{\mathrm{o}} + \Delta\mathbf{s}_{\mathrm{t},m}, \quad \dot{\mathbf{s}}_{\mathrm{t},m} = \dot{\mathbf{s}}_{\mathrm{t},m}^{\mathrm{o}} + \Delta\dot{\mathbf{s}}_{\mathrm{t},m} \tag{1}$$

$$\mathbf{s}_{\mathrm{r},n} = \mathbf{s}_{\mathrm{r},n}^{\mathrm{o}} + \Delta\mathbf{s}_{\mathrm{r},n}, \quad \dot{\mathbf{s}}_{\mathrm{r},n} = \dot{\mathbf{s}}_{\mathrm{r},n}^{\mathrm{o}} + \Delta\dot{\mathbf{s}}_{\mathrm{r},n} \tag{2}$$

where $\Delta\mathbf{s}_{\mathrm{t},m}$, $\Delta\dot{\mathbf{s}}_{\mathrm{t},m}$, $\Delta\mathbf{s}_{\mathrm{r},n}$ and $\Delta\dot{\mathbf{s}}_{\mathrm{r},n}$ represent the error in $\mathbf{s}_{\mathrm{t},m}$, $\dot{\mathbf{s}}_{\mathrm{t},m}$, $\mathbf{s}_{\mathrm{r},n}$ and $\dot{\mathbf{s}}_{\mathrm{r},n}$, respectively. For notation simplicity, we stack the available transmitter and receiver locations together to form a $6(M+N)$-by-1 column vector as $\boldsymbol{\beta} = [\mathbf{s}_{\mathrm{t}}^{\mathrm{T}}, \mathbf{s}_{\mathrm{r}}^{\mathrm{T}}, \dot{\mathbf{s}}_{\mathrm{t}}^{\mathrm{T}}, \dot{\mathbf{s}}_{\mathrm{r}}^{\mathrm{T}}]^{\mathrm{T}}$, where $\mathbf{s}_{\mathrm{t}} = [\mathbf{s}_{\mathrm{t},1}^{\mathrm{T}}, \mathbf{s}_{\mathrm{t},2}^{\mathrm{T}}, \ldots, \mathbf{s}_{\mathrm{t},M}^{\mathrm{T}}]^{\mathrm{T}}$, $\mathbf{s}_{\mathrm{r}} = [\mathbf{s}_{\mathrm{r},1}^{\mathrm{T}}, \mathbf{s}_{\mathrm{r},2}^{\mathrm{T}}, \ldots, \mathbf{s}_{\mathrm{r},N}^{\mathrm{T}}]^{\mathrm{T}}$, $\dot{\mathbf{s}}_{\mathrm{t}} = [\dot{\mathbf{s}}_{\mathrm{t},1}^{\mathrm{T}}, \dot{\mathbf{s}}_{\mathrm{t},2}^{\mathrm{T}}, \ldots, \dot{\mathbf{s}}_{\mathrm{t},M}^{\mathrm{T}}]^{\mathrm{T}}$ and $\dot{\mathbf{s}}_{\mathrm{r}} = [\dot{\mathbf{s}}_{\mathrm{r},1}^{\mathrm{T}}, \dot{\mathbf{s}}_{\mathrm{r},2}^{\mathrm{T}}, \ldots, \dot{\mathbf{s}}_{\mathrm{r},N}^{\mathrm{T}}]^{\mathrm{T}}$. Correspondingly, the actual transmitter and receiver locations are collected in vector form as $\boldsymbol{\beta}^{\mathrm{o}} = [(\mathbf{s}_{\mathrm{t}}^{\mathrm{o}})^{\mathrm{T}}, (\mathbf{s}_{\mathrm{r}}^{\mathrm{o}})^{\mathrm{T}}, (\dot{\mathbf{s}}_{\mathrm{t}}^{\mathrm{o}})^{\mathrm{T}}, (\dot{\mathbf{s}}_{\mathrm{r}}^{\mathrm{o}})^{\mathrm{T}}]^{\mathrm{T}}$ and the related location error vector is given as $\Delta\boldsymbol{\beta} = [\Delta\mathbf{s}_{\mathrm{t}}^{\mathrm{T}}, \Delta\mathbf{s}_{\mathrm{r}}^{\mathrm{T}}, \Delta\dot{\mathbf{s}}_{\mathrm{t}}^{\mathrm{T}}, \Delta\dot{\mathbf{s}}_{\mathrm{r}}^{\mathrm{T}}]^{\mathrm{T}}$. Mathematically, we arrive at

$$\boldsymbol{\beta} = \boldsymbol{\beta}^{\mathrm{o}} + \Delta\boldsymbol{\beta} \tag{3}$$

where the transmitter and receiver location error vector $\Delta\boldsymbol{\beta}$ is assumed follow a Gaussian distribution with zero mean and covariance $\mathbf{Q}_{\boldsymbol{\beta}}$.

The true range and range rate between transmitter m and the target are respectively equal to

$$R_{\mathrm{t},m}^{\mathrm{o}} = ||\mathbf{u}^{\mathrm{o}} - \mathbf{s}_{\mathrm{t},m}^{\mathrm{o}}|| \tag{4}$$

$$\dot{R}_{\mathrm{t},m}^{\mathrm{o}} = \frac{(\mathbf{u}^{\mathrm{o}} - \mathbf{s}_{\mathrm{t},m}^{\mathrm{o}})^{\mathrm{T}}(\dot{\mathbf{u}}^{\mathrm{o}} - \dot{\mathbf{s}}_{\mathrm{t},m}^{\mathrm{o}})}{||\mathbf{u}^{\mathrm{o}} - \mathbf{s}_{\mathrm{t},m}^{\mathrm{o}}||} \tag{5}$$

The true range and range rate between the target and receiver n are respectively equal to

$$R_{\mathrm{r},n}^{\mathrm{o}} = ||\mathbf{u}^{\mathrm{o}} - \mathbf{s}_{\mathrm{r},n}^{\mathrm{o}}|| \tag{6}$$

$$\dot{R}_{\mathrm{r},n}^{\mathrm{o}} = \frac{(\mathbf{u}^{\mathrm{o}} - \mathbf{s}_{\mathrm{r},n}^{\mathrm{o}})^{\mathrm{T}}(\dot{\mathbf{u}}^{\mathrm{o}} - \dot{\mathbf{s}}_{\mathrm{r},n}^{\mathrm{o}})}{||\mathbf{u}^{\mathrm{o}} - \mathbf{s}_{\mathrm{r},n}^{\mathrm{o}}||} \tag{7}$$

By definition, the noise-free BR and BRR for the pair of transmitter m and receiver n are respectively expressed as

$$r^{\mathrm{o}}_{m,n} = R^{\mathrm{o}}_{\mathrm{t},m} + R^{\mathrm{o}}_{\mathrm{r},n} \tag{8}$$
$$\dot{r}^{\mathrm{o}}_{m,n} = \dot{R}^{\mathrm{o}}_{\mathrm{t},m} + \dot{R}^{\mathrm{o}}_{\mathrm{r},n} \tag{9}$$

Due to measurement noises, the noise-free BRs the BRRs are not available, and the available versions are

$$r_{m,n} = r^{\mathrm{o}}_{m,n} + \Delta r_{m,n} \tag{10}$$
$$\dot{r}_{m,n} = \dot{r}^{\mathrm{o}}_{m,n} + \Delta \dot{r}_{m,n} \tag{11}$$

where $\Delta r_{m,n}$ and $\Delta \dot{r}_{m,n}$ represent the BR and BRR measurement noises. For the set of M transmitters and N receivers, (10) and (11) can be cast into two MN-by-1 column vectors as follows:

$$\mathbf{r} = \mathbf{r}^{\mathrm{o}} + \Delta \mathbf{r} \tag{12}$$
$$\dot{\mathbf{r}} = \dot{\mathbf{r}}^{\mathrm{o}} + \Delta \dot{\mathbf{r}} \tag{13}$$

where $\mathbf{r} = [\mathbf{r}_1^{\mathrm{T}}, \mathbf{r}_2^{\mathrm{T}}, \ldots, \mathbf{r}_M^{\mathrm{T}}]^{\mathrm{T}}$ with $\mathbf{r}_m = [r_{m,1}, r_{m,2}, \ldots, r_{m,N}]^{\mathrm{T}}$, $m = 1, 2, \ldots, M$, denotes the vector of measured BRs; $\mathbf{r}^{\mathrm{o}} = [(\mathbf{r}_1^{\mathrm{o}})^{\mathrm{T}}, (\mathbf{r}_2^{\mathrm{o}})^{\mathrm{T}}, \ldots, (\mathbf{r}_M^{\mathrm{o}})^{\mathrm{T}}]^{\mathrm{T}}$ with $\mathbf{r}_m^{\mathrm{o}} = [r^{\mathrm{o}}_{m,1}, r^{\mathrm{o}}_{m,2}, \ldots, r^{\mathrm{o}}_{m,N}]^{\mathrm{T}}$, $m = 1, 2, \ldots, M$, denotes the vector of true BRs; $\Delta \mathbf{r} = [\Delta \mathbf{r}_1^{\mathrm{T}}, \Delta \mathbf{r}_2^{\mathrm{T}}, \ldots, \Delta \mathbf{r}_M^{\mathrm{T}}]^{\mathrm{T}}$ with $\Delta \mathbf{r}_m = [\Delta r_{m,1}, \Delta r_{m,2}, \ldots, \Delta r_{m,N}]^{\mathrm{T}}$, $m = 1, 2, \ldots, M$, denotes the vector of BR measurement noises; $\dot{\mathbf{r}} = [\dot{\mathbf{r}}_1^{\mathrm{T}}, \dot{\mathbf{r}}_2^{\mathrm{T}}, \ldots, \dot{\mathbf{r}}_M^{\mathrm{T}}]^{\mathrm{T}}$ with $\dot{\mathbf{r}}_m = [\dot{r}_{m,1}, \dot{r}_{m,2}, \ldots, \dot{r}_{m,N}]^{\mathrm{T}}$, $m = 1, 2, \ldots, M$, denotes the vector of measured BRRs; $\dot{\mathbf{r}}^{\mathrm{o}} = [(\dot{\mathbf{r}}_1^{\mathrm{o}})^{\mathrm{T}}, (\dot{\mathbf{r}}_2^{\mathrm{o}})^{\mathrm{T}}, \ldots, (\dot{\mathbf{r}}_M^{\mathrm{o}})^{\mathrm{T}}]^{\mathrm{T}}$ with $\dot{\mathbf{r}}_m^{\mathrm{o}} = [\dot{r}^{\mathrm{o}}_{m,1}, \dot{r}^{\mathrm{o}}_{m,2}, \ldots, \dot{r}^{\mathrm{o}}_{m,N}]^{\mathrm{T}}$, $m = 1, 2, \ldots, M$, denotes the vector of true BRRs; $\Delta \dot{\mathbf{r}} = [\Delta \dot{\mathbf{r}}_1^{\mathrm{T}}, \Delta \dot{\mathbf{r}}_2^{\mathrm{T}}, \ldots, \Delta \dot{\mathbf{r}}_M^{\mathrm{T}}]^{\mathrm{T}}$ with $\Delta \dot{\mathbf{r}}_m = [\Delta \dot{r}_{m,1}, \Delta \dot{r}_{m,2}, \ldots, \Delta \dot{r}_{m,N}]^{\mathrm{T}}$, $m = 1, 2, \ldots, M$, denotes the vector of BRR measurement noises.

Collecting the two sets of equations in (12) and (13), yields the total equation set in a $2MN$-by-1 column vector form as

$$\boldsymbol{\alpha} = \boldsymbol{\alpha}^{\mathrm{o}} + \Delta \boldsymbol{\alpha} \tag{14}$$

where $\boldsymbol{\alpha} = [\mathbf{r}^{\mathrm{T}}, \dot{\mathbf{r}}^{\mathrm{T}}]^{\mathrm{T}}$, $\boldsymbol{\alpha}^{\mathrm{o}} = [(\mathbf{r}^{\mathrm{o}})^{\mathrm{T}}, (\dot{\mathbf{r}}^{\mathrm{o}})^{\mathrm{T}}]^{\mathrm{T}}$, $\Delta \boldsymbol{\alpha} = [\Delta \mathbf{r}^{\mathrm{T}}, \Delta \dot{\mathbf{r}}^{\mathrm{T}}]^{\mathrm{T}}$. Without loss of generality, the measurement noise vector $\Delta \boldsymbol{\alpha}$ is modeled as a zero-mean Gaussian vector with covariance matrix $\mathbf{Q}_{\boldsymbol{\alpha}}$.

Different from the localization scenarios in [8]–[10], [15], the localization scenario presented in FIGURE 1 involves K calibration targets, and the BRs/BRRs with respect to these calibration targets are also measured in order to alleviate the transmitter/receiver location uncertainties and enhance the target localization accuracy. The positions and velocities of these calibration targets are denoted by $\mathbf{c}^{\mathrm{o}} = [(\mathbf{c}_1^{\mathrm{o}})^{\mathrm{T}}, (\mathbf{c}_2^{\mathrm{o}})^{\mathrm{T}}, \ldots, (\mathbf{c}_K^{\mathrm{o}})^{\mathrm{T}}]^{\mathrm{T}}$ and $\dot{\mathbf{c}}^{\mathrm{o}} = [(\dot{\mathbf{c}}_1^{\mathrm{o}})^{\mathrm{T}}, (\dot{\mathbf{c}}_2^{\mathrm{o}})^{\mathrm{T}}, \ldots, (\dot{\mathbf{c}}_K^{\mathrm{o}})^{\mathrm{T}}]^{\mathrm{T}}$, where $\mathbf{c}_k^{\mathrm{o}} = [x^{\mathrm{o}}_{\mathrm{c},k}, y^{\mathrm{o}}_{\mathrm{c},k}, z^{\mathrm{o}}_{\mathrm{c},k}]^{\mathrm{T}}$ and $\dot{\mathbf{c}}_k^{\mathrm{o}} = [\dot{x}^{\mathrm{o}}_{\mathrm{c},k}, \dot{y}^{\mathrm{o}}_{\mathrm{c},k}, \dot{z}^{\mathrm{o}}_{\mathrm{c},k}]^{\mathrm{T}}$ represent the position and velocity of calibration target k, $k = 1, 2, \ldots, K$; Similarly, in this study, the positions and velocities of the calibration targets are not known perfectly, and the nominal positions and velocities, denoted by $\mathbf{c}_k = [x_{\mathrm{c},k}, y_{\mathrm{c},k}, z_{\mathrm{c},k}]^{\mathrm{T}}$ and $\dot{\mathbf{c}}_k = [\dot{x}_{\mathrm{c},k}, \dot{y}_{\mathrm{c},k}, \dot{z}_{\mathrm{c},k}]^{\mathrm{T}}$ respectively, are

$$\mathbf{c}_k = \mathbf{c}_k^{\mathrm{o}} + \Delta \mathbf{c}_k \tag{15}$$

$$\dot{\mathbf{c}}_k = \dot{\mathbf{c}}_k^{\mathrm{o}} + \Delta \dot{\mathbf{c}}_k \tag{16}$$

where $\Delta \mathbf{c}_k$ and $\Delta \dot{\mathbf{c}}_k$ represent the position error in $\mathbf{c}_k$ and velocity error in $\dot{\mathbf{c}}_k$, respectively. For the set of K calibration targets, we collect (15) and (16) into a $6K$-by-1 column vector as

$$\boldsymbol{\gamma} = \boldsymbol{\gamma}^{\mathrm{o}} + \Delta \boldsymbol{\gamma} \tag{17}$$

where $\boldsymbol{\gamma} = [\mathbf{c}^{\mathrm{T}}, \dot{\mathbf{c}}^{\mathrm{T}}]^{\mathrm{T}}$ with $\mathbf{c} = [\mathbf{c}_1^{\mathrm{T}}, \mathbf{c}_2^{\mathrm{T}}, \ldots, \mathbf{c}_K^{\mathrm{T}}]^{\mathrm{T}}$ and $\dot{\mathbf{c}} = [\dot{\mathbf{c}}_1^{\mathrm{T}}, \dot{\mathbf{c}}_2^{\mathrm{T}}, \ldots, \dot{\mathbf{c}}_K^{\mathrm{T}}]^{\mathrm{T}}$ represent the vector of nominal calibration target locations, $\boldsymbol{\gamma}^{\mathrm{o}} = [(\mathbf{c}^{\mathrm{o}})^{\mathrm{T}}, (\dot{\mathbf{c}}^{\mathrm{o}})^{\mathrm{T}}]^{\mathrm{T}}$ with $\mathbf{c}^{\mathrm{o}} = [(\mathbf{c}_1^{\mathrm{o}})^{\mathrm{T}}, (\mathbf{c}_2^{\mathrm{o}})^{\mathrm{T}}, \ldots, (\mathbf{c}_K^{\mathrm{o}})^{\mathrm{T}}]^{\mathrm{T}}$ and $\dot{\mathbf{c}}^{\mathrm{o}} = [(\dot{\mathbf{c}}_1^{\mathrm{o}})^{\mathrm{T}}, (\dot{\mathbf{c}}_2^{\mathrm{o}})^{\mathrm{T}}, \ldots, (\dot{\mathbf{c}}_K^{\mathrm{o}})^{\mathrm{T}}]^{\mathrm{T}}$ represent the vector of actual calibration target locations, $\Delta \boldsymbol{\gamma} = [\Delta \mathbf{c}^{\mathrm{T}}, \Delta \dot{\mathbf{c}}^{\mathrm{T}}]^{\mathrm{T}}$ with $\Delta \mathbf{c} = [\Delta \mathbf{c}_1^{\mathrm{T}}, \Delta \mathbf{c}_2^{\mathrm{T}}, \ldots, \Delta \mathbf{c}_K^{\mathrm{T}}]^{\mathrm{T}}$ and $\Delta \dot{\mathbf{c}} = [\Delta \dot{\mathbf{c}}_1^{\mathrm{T}}, \Delta \dot{\mathbf{c}}_2^{\mathrm{T}}, \ldots, \Delta \dot{\mathbf{c}}_K^{\mathrm{T}}]^{\mathrm{T}}$ represent the vector of calibration target location errors. Without loss of generality, $\Delta \boldsymbol{\gamma}$ is assumed to be a zero-mean Gaussian random vector with covariance matrix $\mathbf{Q}_{\boldsymbol{\gamma}}$.

The true range and range rate between transmitter m and calibration target k are respectively equal to

$$R^{\mathrm{o}}_{\mathrm{c},k,\mathrm{t},m} = ||\mathbf{c}_k^{\mathrm{o}} - \mathbf{s}^{\mathrm{o}}_{\mathrm{t},m}|| \tag{18}$$
$$\dot{R}^{\mathrm{o}}_{\mathrm{c},k,\mathrm{t},m} = \frac{(\mathbf{c}_k^{\mathrm{o}} - \mathbf{s}^{\mathrm{o}}_{\mathrm{t},m})^{\mathrm{T}}(\dot{\mathbf{c}}_k^{\mathrm{o}} - \dot{\mathbf{s}}^{\mathrm{o}}_{\mathrm{t},m})}{||\mathbf{c}_k^{\mathrm{o}} - \mathbf{s}^{\mathrm{o}}_{\mathrm{t},m}||} \tag{19}$$

The true range and range rate between calibration target k and receiver n are respectively equal to

$$R^{\mathrm{o}}_{\mathrm{c},k,\mathrm{r},n} = ||\mathbf{c}_k^{\mathrm{o}} - \mathbf{s}^{\mathrm{o}}_{\mathrm{r},n}|| \tag{20}$$
$$\dot{R}^{\mathrm{o}}_{\mathrm{c},k,\mathrm{r},n} = \frac{(\mathbf{c}_k^{\mathrm{o}} - \mathbf{s}^{\mathrm{o}}_{\mathrm{r},n})^{\mathrm{T}}(\dot{\mathbf{c}}_k^{\mathrm{o}} - \dot{\mathbf{s}}^{\mathrm{o}}_{\mathrm{r},n})}{||\mathbf{c}_k^{\mathrm{o}} - \mathbf{s}^{\mathrm{o}}_{\mathrm{r},n}||} \tag{21}$$

The noise-free BR and BRR with respect to calibration target k, transmitter m and receiver n are respectively given by

$$r^{\mathrm{o}}_{\mathrm{c},k,m,n} = R^{\mathrm{o}}_{\mathrm{c},k,\mathrm{t},m} + R^{\mathrm{o}}_{\mathrm{c},k,\mathrm{r},n} \tag{22}$$
$$\dot{r}^{\mathrm{o}}_{\mathrm{c},k,m,n} = \dot{R}^{\mathrm{o}}_{\mathrm{c},k,\mathrm{t},m} + \dot{R}^{\mathrm{o}}_{\mathrm{c},k,\mathrm{r},n} \tag{23}$$

In the presence of measurement noises, the corresponding BR and BRR measurements can be modeled as

$$r_{\mathrm{c},k,m,n} = r^{\mathrm{o}}_{\mathrm{c},k,m,n} + \Delta r_{\mathrm{c},k,m,n} \tag{24}$$
$$\dot{r}_{\mathrm{c},k,m,n} = \dot{r}^{\mathrm{o}}_{\mathrm{c},k,m,n} + \Delta \dot{r}_{\mathrm{c},k,m,n} \tag{25}$$

where $\Delta r_{\mathrm{c},k,m,n}$ and $\Delta \dot{r}_{\mathrm{c},k,m,n}$ are the BR and BRR measurement noises. With respect to the K calibration targets, M transmitters and N receivers, we can collect (24) and (25) into two KMN-by-1 column vectors as

$$\mathbf{r}_{\mathrm{c}} = \mathbf{r}_{\mathrm{c}}^{\mathrm{o}} + \Delta \mathbf{r}_{\mathrm{c}} \tag{26}$$
$$\dot{\mathbf{r}}_{\mathrm{c}} = \dot{\mathbf{r}}_{\mathrm{c}}^{\mathrm{o}} + \Delta \dot{\mathbf{r}}_{\mathrm{c}} \tag{27}$$

where $\mathbf{r}_{\mathrm{c}} = [\mathbf{r}_{\mathrm{c},1}^{\mathrm{T}}, \mathbf{r}_{\mathrm{c},2}^{\mathrm{T}}, \ldots, \mathbf{r}_{\mathrm{c},K}^{\mathrm{T}}]^{\mathrm{T}}$ with $\mathbf{r}_{\mathrm{c},k} = [\mathbf{r}_{\mathrm{c},k,1}^{\mathrm{T}}, \mathbf{r}_{\mathrm{c},k,2}^{\mathrm{T}}, \ldots, \mathbf{r}_{\mathrm{c},k,M}^{\mathrm{T}}]^{\mathrm{T}}$ and $\mathbf{r}_{\mathrm{c},k,m} = [r_{\mathrm{c},k,m,1}, r_{\mathrm{c},k,m,2}, \ldots, r_{\mathrm{c},k,m,N}]^{\mathrm{T}}$ denotes the vector of measured BRs from the calibration targets; $\mathbf{r}_{\mathrm{c}}^{\mathrm{o}} = [(\mathbf{r}_{\mathrm{c},1}^{\mathrm{o}})^{\mathrm{T}}, (\mathbf{r}_{\mathrm{c},2}^{\mathrm{o}})^{\mathrm{T}}, \ldots, (\mathbf{r}_{\mathrm{c},K}^{\mathrm{o}})^{\mathrm{T}}]^{\mathrm{T}}$ with $\mathbf{r}_{\mathrm{c},k}^{\mathrm{o}} = [(\mathbf{r}_{\mathrm{c},k,1}^{\mathrm{o}})^{\mathrm{T}}, (\mathbf{r}_{\mathrm{c},k,2}^{\mathrm{o}})^{\mathrm{T}}, \ldots, (\mathbf{r}_{\mathrm{c},k,M}^{\mathrm{o}})^{\mathrm{T}}]^{\mathrm{T}}$ and $\mathbf{r}_{\mathrm{c},k,m}^{\mathrm{o}} = [r^{\mathrm{o}}_{\mathrm{c},k,m,1}, r^{\mathrm{o}}_{\mathrm{c},k,m,2}, \ldots, r^{\mathrm{o}}_{\mathrm{c},k,m,N}]^{\mathrm{T}}$ denotes the vector of true BRs from

the calibration targets; $\Delta\mathbf{r}_c = [\Delta\mathbf{r}_{c,1}^T, \Delta\mathbf{r}_{c,2}^T, \ldots, \Delta\mathbf{r}_{c,K}^T]^T$ with $\Delta\mathbf{r}_{c,k} = [\Delta\mathbf{r}_{c,k,1}^T, \Delta\mathbf{r}_{c,k,2}^T, \ldots, \Delta\mathbf{r}_{c,k,M}^T]^T$ and $\Delta\mathbf{r}_{c,k,m} = [\Delta r_{c,k,m,1}, \Delta r_{c,k,m,2}, \ldots, \Delta r_{c,k,m,N}]^T$ denotes the corresponding BR measurement noise vector; $\dot{\mathbf{r}}_c = [\dot{\mathbf{r}}_{c,1}^T, \dot{\mathbf{r}}_{c,2}^T, \ldots, \dot{\mathbf{r}}_{c,K}^T]^T$ with $\dot{\mathbf{r}}_{c,k} = [\dot{\mathbf{r}}_{c,k,1}^T, \dot{\mathbf{r}}_{c,k,2}^T, \ldots, \dot{\mathbf{r}}_{c,k,M}^T]^T$ and $\dot{\mathbf{r}}_{c,k,m} = [\dot{r}_{c,k,m,1}, \dot{r}_{c,k,m,2}, \ldots, \dot{r}_{c,k,m,N}]^T$ denotes the vector of measured BRRs from the calibration targets; $\dot{\mathbf{r}}_c^o = [(\dot{\mathbf{r}}_{c,1}^o)^T, (\dot{\mathbf{r}}_{c,2}^o)^T, \ldots, (\dot{\mathbf{r}}_{c,K}^o)^T]^T$ with $\dot{\mathbf{r}}_{c,k}^o = [(\dot{\mathbf{r}}_{c,k,1}^o)^T, (\dot{\mathbf{r}}_{c,k,2}^o)^T, \ldots, (\dot{\mathbf{r}}_{c,k,M}^o)^T]^T$ and $\dot{\mathbf{r}}_{c,k,m}^o = [\dot{r}_{c,k,m,1}^o, \dot{r}_{c,k,m,2}^o, \ldots, \dot{r}_{c,k,m,N}^o]^T$ denotes the vector of true BRRs from the calibration targets; $\Delta\dot{\mathbf{r}}_c = [\Delta\dot{\mathbf{r}}_{c,1}^T, \Delta\dot{\mathbf{r}}_{c,2}^T, \ldots, \Delta\dot{\mathbf{r}}_{c,K}^T]^T$ with $\Delta\dot{\mathbf{r}}_{c,k} = [\Delta\dot{\mathbf{r}}_{c,k,1}^T, \Delta\dot{\mathbf{r}}_{c,k,2}^T, \ldots, \Delta\dot{\mathbf{r}}_{c,k,M}^T]^T$ and $\Delta\dot{\mathbf{r}}_{c,k,m} = [\Delta\dot{r}_{c,k,m,1}, \Delta\dot{r}_{c,k,m,2}, \ldots, \Delta\dot{r}_{c,k,m,N}]^T$ denotes the corresponding BRR measurement noise vector.

Putting the two sets of equations in (26) and (27) together, yields the total equation set in a $2KMN$-by-1 column vector form as

$$\boldsymbol{\alpha}_c = \boldsymbol{\alpha}_c^o + \Delta\boldsymbol{\alpha}_c \tag{28}$$

where $\boldsymbol{\alpha}_c = [\mathbf{r}_c^T, \dot{\mathbf{r}}_c^T]^T$, $\boldsymbol{\alpha}_c^o = [(\mathbf{r}_c^o)^T, (\dot{\mathbf{r}}_c^o)^T]^T$, $\Delta\boldsymbol{\alpha}_c = [\Delta\mathbf{r}_c^T, \Delta\dot{\mathbf{r}}_c^T]^T$. The total measurement noise vector $\Delta\boldsymbol{\alpha}_c$ is modeled as a zero-mean Gaussian vector with covariance matrix $\mathbf{Q}_{\boldsymbol{\alpha}c}$.

In this study, we shall estimate the target location vector $\boldsymbol{\theta}^o = [(\mathbf{u}^o)^T, (\dot{\mathbf{u}}^o)^T]^T$ as accurately as possible using the BR and BRR measurement vector $\boldsymbol{\alpha}$ from the unknown target together with the noisy transmitter and receiver location vector $\boldsymbol{\beta}$. Different from existing studies, the calibration targets with nominal location vector $\boldsymbol{\gamma}$ and the corresponding BR and BRR vector $\boldsymbol{\alpha}_c$ are also employed to improve the target localization accuracy.

III. ANALYSIS OF CRLB WITH CALIBRATION TARGETS

We shall first characterize the best achievable localization accuracy with the use of calibration targets by establishing the CRLB for the target location estimation. In addition to the BR and BRR measurement noises, the presence of errors in the transmitter/receiver/calibration target locations are also included. The localization accuracy improvement brought by the use of calibration targets will be characterized through the comparison between the CRLB with the calibration targets and the one without.

The deterministic unknowns for the CRLB evaluation, including the unknown target location $\boldsymbol{\theta}^o$, the actual transmitter and receiver location vector $\boldsymbol{\beta}^o$ and the actual calibration target location vector $\boldsymbol{\gamma}^o$, are cast into a $6(M+N+K+1)$-by-1 column vector as $\boldsymbol{\varphi}^o = [(\boldsymbol{\theta}^o)^T, (\boldsymbol{\beta}^o)^T, (\boldsymbol{\gamma}^o)^T]^T$. The observations for the CRLB evaluation, including the BR and BRR measurement vector $\boldsymbol{\alpha}$ from the unknown target, the BR and BRR measurement vector $\boldsymbol{\alpha}_c$ from the calibration targets, the nominal transmitter and receiver location vector $\boldsymbol{\beta}$ and the nominal calibration target location vector $\boldsymbol{\gamma}$, are cast into a $(2MN + 2MNK + 6M + 6N + 6K)$-by-1 column vector as $z = [\boldsymbol{\alpha}^T, \boldsymbol{\alpha}_c^T, \boldsymbol{\beta}^T, \boldsymbol{\gamma}^T]^T$. From the error assumptions given in Section II, the joint probability density function (pdf) of $\mathbf{z}$ given $\boldsymbol{\varphi}^o$ is readily shown to be

$$\begin{aligned} &p(z|\boldsymbol{\varphi}^o) \\ &= p(\boldsymbol{\alpha}|\boldsymbol{\theta}^o, \boldsymbol{\beta}^o) \cdot p(\boldsymbol{\alpha}_c|\boldsymbol{\beta}^o, \boldsymbol{\gamma}^o) \cdot p(\boldsymbol{\beta}|\boldsymbol{\beta}^o) \cdot p(\boldsymbol{\gamma}|\boldsymbol{\gamma}^o) \\ &= \kappa \cdot \exp\left[-\frac{1}{2}(\boldsymbol{\alpha}-\boldsymbol{\alpha}^o)^T\mathbf{Q}_{\boldsymbol{\alpha}}^{-1}(\boldsymbol{\alpha}-\boldsymbol{\alpha}^o)\right. \\ &\quad -\frac{1}{2}(\boldsymbol{\beta}-\boldsymbol{\beta}^o)^T\mathbf{Q}_{\boldsymbol{\beta}}^{-1}(\boldsymbol{\beta}-\boldsymbol{\beta}^o) - \frac{1}{2}(\boldsymbol{\beta}-\boldsymbol{\beta}^o)^T\mathbf{Q}_{\boldsymbol{\beta}}^{-1}(\boldsymbol{\beta}-\boldsymbol{\beta}^o) \\ &\quad \left.-\frac{1}{2}(\boldsymbol{\gamma}-\boldsymbol{\gamma}^o)^T\mathbf{Q}_{\boldsymbol{\gamma}}^{-1}(\boldsymbol{\gamma}-\boldsymbol{\gamma}^o)\right] \end{aligned} \tag{29}$$

where κ is constant independent of the unknowns. By definition, the $6(M+N+K+1)$-by-$6(M+N+K+1)$ Fisher information matrix is structured as

$$\begin{aligned} \mathbf{FIM}(\boldsymbol{\varphi}^o) &\triangleq \mathrm{E}\left[\frac{\partial \ln p(\mathbf{z}|\boldsymbol{\varphi}^o)}{\partial\boldsymbol{\varphi}^o}\left(\frac{\partial \ln p(\mathbf{z}|\boldsymbol{\varphi}^o)}{\partial\boldsymbol{\varphi}^o}\right)\right] \\ &= \begin{bmatrix} \mathbf{X} & \mathbf{Y} & \mathbf{O}_{6\times6} \\ \mathbf{Y}^T & \mathbf{Z} & \mathbf{R}^T \\ \mathbf{O}_{6\times6} & \mathbf{R} & \mathbf{P} \end{bmatrix} \end{aligned} \tag{30}$$

where the blocks $\mathbf{X}$, $\mathbf{Y}$, $\mathbf{Z}$, $\mathbf{R}$ and $\mathbf{P}$ are

$$\mathbf{X} = \left(\frac{\partial\boldsymbol{\alpha}^o}{\partial\boldsymbol{\theta}^o}\right)^T\mathbf{Q}_{\boldsymbol{\alpha}}^{-1}\left(\frac{\partial\boldsymbol{\alpha}^o}{\partial\boldsymbol{\theta}^o}\right) \tag{31}$$

$$\mathbf{Y} = \left(\frac{\partial\boldsymbol{\alpha}^o}{\partial\boldsymbol{\theta}^o}\right)^T\mathbf{Q}_{\boldsymbol{\alpha}}^{-1}\left(\frac{\partial\boldsymbol{\alpha}^o}{\partial\boldsymbol{\beta}^o}\right) \tag{32}$$

$$\begin{aligned} \mathbf{Z} = \mathbf{Q}_{\boldsymbol{\beta}}^{-1} &+ \left(\frac{\partial\boldsymbol{\alpha}^o}{\partial\boldsymbol{\beta}^o}\right)^T\mathbf{Q}_{\boldsymbol{\alpha}}^{-1}\left(\frac{\partial\boldsymbol{\alpha}^o}{\partial\boldsymbol{\beta}^o}\right) \\ &+ \left(\frac{\partial\boldsymbol{\alpha}_c^o}{\partial\boldsymbol{\beta}^o}\right)^T\mathbf{Q}_{\boldsymbol{\alpha}c}^{-1}\left(\frac{\partial\boldsymbol{\alpha}_c^o}{\partial\boldsymbol{\beta}^o}\right) \end{aligned} \tag{33}$$

$$\mathbf{R} = \left(\frac{\partial\boldsymbol{\alpha}_c^o}{\partial\boldsymbol{\gamma}^o}\right)^T\mathbf{Q}_{\boldsymbol{\alpha}c}^{-1}\left(\frac{\partial\boldsymbol{\alpha}_c^o}{\partial\boldsymbol{\beta}^o}\right) \tag{34}$$

$$\mathbf{P} = \mathbf{Q}_{\boldsymbol{\gamma}}^{-1} + \left(\frac{\partial\boldsymbol{\alpha}_c^o}{\partial\boldsymbol{\gamma}^o}\right)^T\mathbf{Q}_{\boldsymbol{\alpha}c}^{-1}\left(\frac{\partial\boldsymbol{\alpha}_c^o}{\partial\boldsymbol{\gamma}^o}\right) \tag{35}$$

The explicit expressions for the partial derivatives $\partial\boldsymbol{\alpha}^o/\partial\boldsymbol{\theta}^o$, $\partial\boldsymbol{\alpha}^o/\partial\boldsymbol{\beta}^o$, $\partial\boldsymbol{\alpha}_c^o/\partial\boldsymbol{\beta}^o$ and $\partial\boldsymbol{\alpha}_c^o/\partial\boldsymbol{\gamma}^o$ are detailed in Appendix.

Form (30), it follows that the CRLB of $\boldsymbol{\varphi}^o$, denoted by $\mathbf{CRLB}_c(\boldsymbol{\varphi}^o)$, can be obtained as $\mathbf{FIM}(\boldsymbol{\varphi}^o)^{-1}$. However, we are only interested in the bound on the target location parameters $\boldsymbol{\theta}^o$, given by the upper left 6-by-6 block of $\mathbf{FIM}(\boldsymbol{\varphi}^o)^{-1}$. This block, denoted by $\mathbf{CRLB}_c(\boldsymbol{\theta}^o)$, can be obtained from a matrix of this form by exploiting the partitioned matrix inversion formula and the matrix inversion lemma [23], as

$$\begin{aligned} \mathbf{CRLB}_c(\boldsymbol{\theta}^o) = \mathbf{X}^{-1} + \mathbf{X}^{-1}\mathbf{Y}(\mathbf{Z} - \mathbf{Y}^T\mathbf{X}^{-1}\mathbf{Y} \\ - \mathbf{R}^T\mathbf{P}^{-1}\mathbf{R})^{-1}\mathbf{Y}^T\mathbf{X}^{-1} \end{aligned} \tag{36}$$

Next, we shall characterize localization accuracy improvement brought by the use of calibration targets through the comparison between the CRLB with the calibration targets and the one without. For this purpose, the CRLB of $\boldsymbol{\theta}^o$ with transmitter/receiver location uncertainties but without calibration derived in [15], denoted by $\mathbf{CRLB}_s(\boldsymbol{\theta}^o)$, is presented

below

$$\mathbf{CRLB}_{\mathrm{s}}(\mathbf{u}^{\mathrm{o}})=\mathbf{X}^{-1}+\mathbf{X}^{-1}\mathbf{Y}(\widehat{\mathbf{Z}}-\mathbf{Y}^{\mathrm{T}}\mathbf{X}^{-1}\mathbf{Y})^{-1}\mathbf{Y}^{\mathrm{T}}\mathbf{X}^{-1} \quad (37)$$

where $\widehat{\mathbf{Z}} = \mathbf{Q}_{\boldsymbol{\beta}}^{-1} + (\partial\boldsymbol{\alpha}^{\mathrm{o}}/\partial\boldsymbol{\beta}^{\mathrm{o}})^{\mathrm{T}}\mathbf{Q}_{\boldsymbol{\alpha}}^{-1}(\partial\boldsymbol{\alpha}^{\mathrm{o}}/\partial\boldsymbol{\beta}^{\mathrm{o}})$. It may be interesting to note, that there are structural similarities between the two CRLBs in (36) and (37). To illustrate, let us define $\check{\mathbf{Z}} = \mathbf{Z} - \mathbf{R}^{\mathrm{T}}\mathbf{P}^{-1}\mathbf{R}$. By exploiting the expressions of $\mathbf{Z}$, $\mathbf{R}$ and $\mathbf{P}$ in (33)-(35), invoking the matrix inversion lemma [23] to the term $(\partial\boldsymbol{\alpha}_{\mathrm{c}}^{\mathrm{o}}/\partial\boldsymbol{\beta}^{\mathrm{o}})^{\mathrm{T}}\mathbf{Q}_{\boldsymbol{\alpha}\mathrm{c}}^{-1}(\partial\boldsymbol{\alpha}_{\mathrm{c}}^{\mathrm{o}}/\partial\boldsymbol{\beta}^{\mathrm{o}}) - \mathbf{R}^{\mathrm{T}}\mathbf{P}^{-1}\mathbf{R}$ and then simplifying, we can rewrite $\check{\mathbf{Z}}$ as

$$\begin{aligned}\check{\mathbf{Z}} = \mathbf{Q}_{\boldsymbol{\beta}}^{-1} &+ \left(\frac{\partial\boldsymbol{\alpha}^{\mathrm{o}}}{\partial\boldsymbol{\beta}^{\mathrm{o}}}\right)^{\mathrm{T}}\mathbf{Q}_{\boldsymbol{\alpha}}^{-1}\left(\frac{\partial\boldsymbol{\alpha}^{\mathrm{o}}}{\partial\boldsymbol{\beta}^{\mathrm{o}}}\right)\\ &+\left(\frac{\partial\boldsymbol{\alpha}_{\mathrm{c}}^{\mathrm{o}}}{\partial\boldsymbol{\beta}^{\mathrm{o}}}\right)^{\mathrm{T}}\left(\mathbf{Q}_{\boldsymbol{\alpha}\mathrm{c}}+\left(\frac{\partial\boldsymbol{\alpha}_{\mathrm{c}}^{\mathrm{o}}}{\partial\boldsymbol{\gamma}^{\mathrm{o}}}\right)\mathbf{Q}_{\boldsymbol{\gamma}}\left(\frac{\partial\boldsymbol{\alpha}_{\mathrm{c}}^{\mathrm{o}}}{\partial\boldsymbol{\gamma}^{\mathrm{o}}}\right)^{\mathrm{T}}\right)^{-1}\left(\frac{\partial\boldsymbol{\alpha}_{\mathrm{c}}^{\mathrm{o}}}{\partial\boldsymbol{\beta}^{\mathrm{o}}}\right)\end{aligned} \quad (38)$$

Plugging $\check{\mathbf{Z}}$ into (36) yields an equivalent representation of $\mathbf{CRLB}_{\mathrm{c}}(\boldsymbol{\theta}^{\mathrm{o}})$ as

$$\mathbf{CRLB}_{\mathrm{c}}(\boldsymbol{\theta}^{\mathrm{o}})=\mathbf{X}^{-1}+\mathbf{X}^{-1}\mathbf{Y}(\check{\mathbf{Z}}-\mathbf{Y}^{\mathrm{T}}\mathbf{X}^{-1}\mathbf{Y})^{-1}\mathbf{Y}^{\mathrm{T}}\mathbf{X}^{-1} \quad (39)$$

Now, the two CRLBs in (37) and (39) are evidently identical in structure, except that $\check{\mathbf{Z}}$ is substituted by $\widehat{\mathbf{Z}}$. This implies, as could be expected, the use of calibration targets introduces an additional component in the big matrix within the parentheses as

$$\begin{aligned}\tilde{\mathbf{Z}} &= \check{\mathbf{Z}} - \widehat{\mathbf{Z}}\\ &= \left(\frac{\partial\boldsymbol{\alpha}_{\mathrm{c}}^{\mathrm{o}}}{\partial\boldsymbol{\beta}^{\mathrm{o}}}\right)^{\mathrm{T}}\mathbf{Q}_{\boldsymbol{\alpha}\mathrm{c}}^{-1}\left(\frac{\partial\boldsymbol{\alpha}_{\mathrm{c}}^{\mathrm{o}}}{\partial\boldsymbol{\beta}^{\mathrm{o}}}\right) - \mathbf{R}^{\mathrm{T}}\mathbf{P}^{-1}\mathbf{R}\\ &= \left(\frac{\partial\boldsymbol{\alpha}_{\mathrm{c}}^{\mathrm{o}}}{\partial\boldsymbol{\beta}^{\mathrm{o}}}\right)^{\mathrm{T}}\left(\mathbf{Q}_{\boldsymbol{\alpha}\mathrm{c}}+\left(\frac{\partial\boldsymbol{\alpha}_{\mathrm{c}}^{\mathrm{o}}}{\partial\boldsymbol{\gamma}^{\mathrm{o}}}\right)\mathbf{Q}_{\boldsymbol{\gamma}}\left(\frac{\partial\boldsymbol{\alpha}_{\mathrm{c}}^{\mathrm{o}}}{\partial\boldsymbol{\gamma}^{\mathrm{o}}}\right)^{\mathrm{T}}\right)^{-1}\\ &\quad\times\left(\frac{\partial\boldsymbol{\alpha}_{\mathrm{c}}^{\mathrm{o}}}{\partial\boldsymbol{\beta}^{\mathrm{o}}}\right)\end{aligned} \quad (40)$$

Rearranging $(\check{Z} - \mathbf{Y}^{\mathrm{T}}\mathbf{X}^{-1}\mathbf{Y})^{-1}$ in (39) as $((\widehat{\mathbf{Z}} - \mathbf{Y}^{\mathrm{T}}\mathbf{X}^{-1}\mathbf{Y}) + \tilde{\mathbf{Z}})^{-1}$ and invoking the matrix inversion lemma [23] to the term $((\widehat{\mathbf{Z}} - \mathbf{Y}^{\mathrm{T}}\mathbf{X}^{-1}\mathbf{Y}) + \tilde{\mathbf{Z}})^{-1}$, we have after tedious mathematical manipulations,

$$\mathbf{CRLB}_{\mathrm{s}}(\boldsymbol{\theta}^{\mathrm{o}}) - \mathbf{CRLB}_{\mathrm{c}}(\boldsymbol{\theta}^{\mathrm{o}}) = \mathbf{X}^{-1}\mathbf{Y}\boldsymbol{\Gamma}\mathbf{Y}^{\mathrm{T}}\mathbf{X}^{-1} \quad (41)$$

where $\boldsymbol{\Gamma} = \mathbf{H}^{-1}\boldsymbol{\Upsilon}(\mathbf{I} + \boldsymbol{\Upsilon}^{\mathrm{T}}\mathbf{H}^{-1}\boldsymbol{\Upsilon})^{-1}\boldsymbol{\Upsilon}^{\mathrm{T}}\mathbf{H}^{-1}$, $\mathbf{H} = \check{\mathbf{Z}} - \mathbf{Y}^{\mathrm{T}}\mathbf{X}^{-1}\mathbf{Y}$, and $\boldsymbol{\Upsilon} = (\partial\boldsymbol{\alpha}_{\mathrm{c}}^{\mathrm{o}}/\partial\boldsymbol{\beta}^{\mathrm{o}})^{\mathrm{T}}\mathbf{L}_{\boldsymbol{\alpha}\mathrm{c}}$ with $\mathbf{L}_{\boldsymbol{\alpha}\mathrm{c}}$ being the Cholesky decomposition of $(\mathbf{Q}_{\boldsymbol{\alpha}\mathrm{c}} + (\partial\boldsymbol{\alpha}_{\mathrm{c}}^{\mathrm{o}}/\partial\boldsymbol{\gamma}^{\mathrm{o}})\mathbf{Q}_{\boldsymbol{\gamma}}(\partial\boldsymbol{\alpha}_{\mathrm{c}}^{\mathrm{o}}/\partial\boldsymbol{\gamma}^{\mathrm{o}})^{\mathrm{T}})^{-1}$, i.e., $\mathbf{L}_{\boldsymbol{\alpha}\mathrm{c}}\mathbf{L}_{\boldsymbol{\alpha}\mathrm{c}}^{\mathrm{T}} = (\mathbf{Q}_{\boldsymbol{\alpha}\mathrm{c}} + (\partial\boldsymbol{\alpha}_{\mathrm{c}}^{\mathrm{o}}/\partial\boldsymbol{\gamma}^{\mathrm{o}})\mathbf{Q}_{\boldsymbol{\gamma}}(\partial\boldsymbol{\alpha}_{\mathrm{c}}^{\mathrm{o}}/\partial\boldsymbol{\gamma}^{\mathrm{o}})^{\mathrm{T}})^{-1}$. As evident from the structural form of (41), the right side is just the performance enhancement from the use of calibration targets. It is positive semi-definite (PSD) since it has a symmetric structure and $\boldsymbol{\Upsilon}^{\mathrm{T}}$ is not full column rank. Even if the nominal locations of calibration targets and the corresponding BR/BRR measurements are very erroneous, (41) can still remain PSD. In theory, only in the edge case when $(\mathbf{Q}_{\boldsymbol{\alpha}\mathrm{c}} + (\partial\boldsymbol{\alpha}_{\mathrm{c}}^{\mathrm{o}}/\partial\boldsymbol{\gamma}^{\mathrm{o}})\mathbf{Q}_{\boldsymbol{\gamma}}(\partial\boldsymbol{\alpha}_{\mathrm{c}}^{\mathrm{o}}/\partial\boldsymbol{\gamma}^{\mathrm{o}})^{\mathrm{T}})^{-1}$ tends to zero and then $\mathbf{L}_{\boldsymbol{\alpha}\mathrm{c}} \to \mathbf{O}$ and $\boldsymbol{\Upsilon} \to \mathbf{O}$, the performance enhancement in (41) would tend to zero. However, this edge case hardly exists in reality. Hence, mathematically, we have

$$\mathbf{CRLB}_{\mathrm{s}}(\boldsymbol{\theta}^{\mathrm{o}}) \geq \mathbf{CRLB}_{\mathrm{c}}(\boldsymbol{\theta}^{\mathrm{o}}) \quad (42)$$

The matrix inequality $\mathbf{A} \geq \mathbf{B}$ implies that $\mathbf{A} - \mathbf{B}$ is PSD, from which $\mathrm{tr}(\mathbf{CRLB}_{\mathrm{s}}(\boldsymbol{\theta}^{\mathrm{o}})) \geq \mathrm{tr}(\mathbf{CRLB}_{\mathrm{c}}(\boldsymbol{\theta}^{\mathrm{o}}))$ can be inferred. In a physical sense, the trace of $\mathbf{CRLB}_{\mathrm{c}}(\boldsymbol{\theta}^{\mathrm{o}})$ and $\mathbf{CRLB}_{\mathrm{s}}(\boldsymbol{\theta}^{\mathrm{o}})$ respectively denotes the minimum possible mean-square localization error for the unknown target with and without using calibration targets. Hence, it can be concluded that using calibration targets brings potential enhancement to the target localization accuracy, at least at the CRLB level.

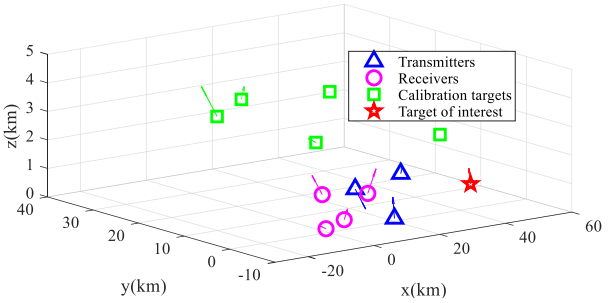

FIGURE 2. MPR localization scenario geometry for simulation.

TABLE 1. Positions (in meters) and velocities (in meters/second) of the transmitters, receivers and calibration targets.

transmitters	$x_{t,m}^{\mathrm{o}}$	$y_{t,m}^{\mathrm{o}}$	$z_{t,m}^{\mathrm{o}}$	$\dot{x}_{t,m}^{\mathrm{o}}$	$\dot{y}_{t,m}^{\mathrm{o}}$	$\dot{z}_{t,m}^{\mathrm{o}}$
1	20000	0	100	200	200	100
2	15000	5000	1000	200	-200	-100
3	15000	-5000	2000	-200	-200	50
receivers	$x_{r,n}^{\mathrm{o}}$	$y_{r,n}^{\mathrm{o}}$	$z_{r,n}^{\mathrm{o}}$	$\dot{x}_{r,n}^{\mathrm{o}}$	$\dot{y}_{r,n}^{\mathrm{o}}$	$\dot{z}_{r,n}^{\mathrm{o}}$
1	2000	2000	0	100	300	0
2	2000	-2000	500	300	100	50
3	5000	5000	1000	-100	300	100
4	5000	-5000	1500	300	-100	150
Calibration targets	$x_{c,k}^{\mathrm{o}}$	$y_{c,k}^{\mathrm{o}}$	$z_{c,k}^{\mathrm{o}}$	$\dot{x}_{c,k}^{\mathrm{o}}$	$\dot{y}_{c,k}^{\mathrm{o}}$	$\dot{z}_{c,k}^{\mathrm{o}}$
1	10000	10000	2500	200	400	0
2	15000	30000	3000	400	200	50
3	20000	-10000	3500	200	-200	-50
4	-20000	10000	4000	-200	200	100
5	-1000	-1000	5000	-200	-200	100

Example 1: In order to verify the above analysis of the CRLB, a numerical example using the localization geometry given in FIGURE 2, was performed. The MPR system equipped with $M = 3$ transmitters, $N = 4$ receivers and $K = 5$ calibration targets, is deployed to determine the unknown target position $\mathbf{u}^{\mathrm{o}} = [50000, 5000, 500]^{\mathrm{T}}$m and velocity $\dot{\mathbf{u}}^{\mathrm{o}} = [300, 300, 100]^{\mathrm{T}}$m/s using BR and BRR measurements. The positions and velocities of the transmitters/receivers/calibration targets are tabulated in TABLE 1. The noise covariance matrix of the BR and BRR measurements from the unknown target is $\mathbf{Q}_{\boldsymbol{\alpha}} = \mathrm{diag}\{\sigma_{\boldsymbol{\alpha}}^2\mathbf{I}_{MN}, 0.01\sigma_{\boldsymbol{\alpha}}^2\mathbf{I}_{MN}\}$, where $\sigma_{\boldsymbol{\alpha}}$ reflects BR and BRR

measurement noise level; The covariance matrix of the transmitter/receiver location error is given as $\mathbf{Q}_{\boldsymbol{\beta}} = \text{diag}\{\sigma_{\boldsymbol{\beta}}^2\mathbf{I}_{3(M+N)}, 0.01\sigma_{\boldsymbol{\beta}}^2\mathbf{I}_{3(M+N)}\}$ where $\sigma_{\boldsymbol{\beta}}$ reflects the transmitter/receiver location uncertainty level; The covariance matrix of calibration target location error is $\mathbf{Q}_{\boldsymbol{\gamma}} = diag\{\sigma_{\boldsymbol{\gamma}}^2\mathbf{I}_{3K}, 0.01\sigma_{\boldsymbol{\gamma}}^2\mathbf{I}_{3K}\}$ where $\sigma_{\boldsymbol{\gamma}}$ reflects the calibration target location error level; The covariance matrix of the calibration BR and BR measurement noise is $\mathbf{Q}_{\boldsymbol{\alpha}\text{c}} = \text{diag}\{\sigma_{\boldsymbol{\alpha}\text{c}}^2\mathbf{I}_{KMN}, 0.01\sigma_{\boldsymbol{\alpha}\text{c}}^2\mathbf{I}_{KMN}\}$ where $\sigma_{\boldsymbol{\alpha}\text{c}} = \sigma_{\boldsymbol{\alpha}}$ reflects the calibration BR and BRR measurement noise level. The difference between the target localization CRLB with and without the use of calibration targets is illustrated in FIGURE 3.

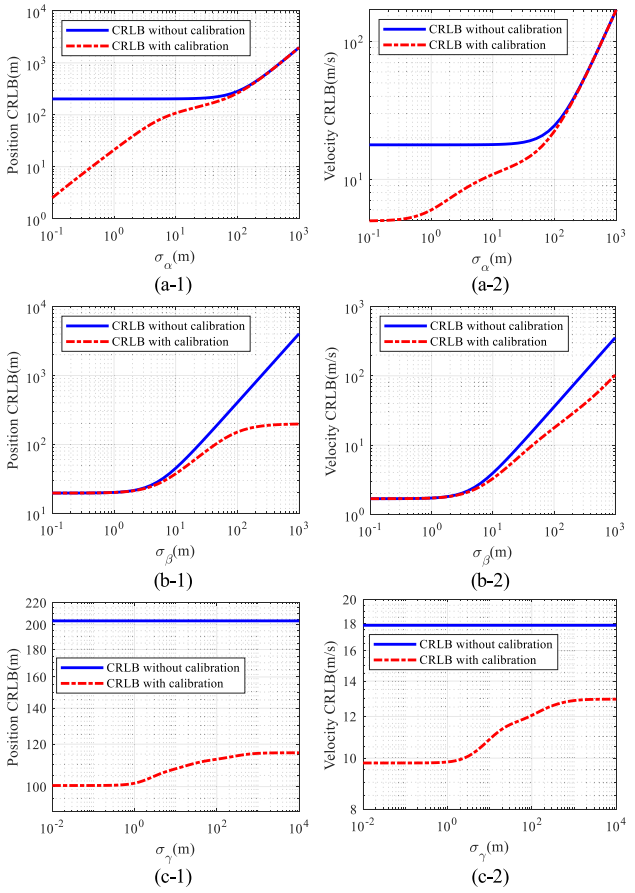

FIGURE 3. Comparison of the CRLBs with and without using calibration targets: (a-1) position CRLB versus BR measurement noise level $\sigma_{\boldsymbol{\alpha}}$; (a-2) velocity CRLB versus BR measurement noise level $\sigma_{\boldsymbol{\alpha}}$; (b-1) position CRLB versus transmitter and receiver location uncertainty level $\sigma_{\boldsymbol{\beta}}$; (b-2) velocity CRLB versus transmitter and receiver location uncertainty level $\sigma_{\boldsymbol{\beta}}$; (c-1) position CRLB versus calibration target location error level $\sigma_{\boldsymbol{\gamma}}$; (c-2) velocity CRLB versus calibration target location error level $\sigma_{\boldsymbol{\gamma}}$.

FIGURE 3(a) plots the traces of $\mathbf{CRLB}_{\text{c}}(\boldsymbol{\theta}^{\text{o}})$ and $\mathbf{CRLB}_{\text{s}}(\boldsymbol{\theta}^{\text{o}})$ as $\sigma_{\boldsymbol{\alpha}}$ increases from 10^{-1}m to 10^{3}m while the transmitter/receiver location uncertainty level and calibration target location error level are fixed at $\sigma_{\boldsymbol{\beta}} = 50$m and $\sigma_{\boldsymbol{\gamma}} = 10$m respectively. It can be observed from FIGURE 3(a) that the CRLB with calibration targets is generally below the one without, which coincides with the analytical conclusion given in (42). However, in the edge case where the BR and BRR measurement noise is very large, two CRLBs would tend to be the same. This is because in this case, the BR and BRR measurement noise dominates and the effect of transmitter/receiver location uncertainties on the localization accuracy is relatively small. FIGURE 3(b) depicts the traces of $\mathbf{CRLB}_{\text{c}}(\boldsymbol{\theta}^{\text{o}})$ and $\mathbf{CRLB}_{\text{s}}(\boldsymbol{\theta}^{\text{o}})$ as the transmitter/receiver location uncertainty level $\sigma_{\boldsymbol{\beta}}$ increases while the BR/BRR measurement noise level and calibration target location error level are fixed at $\sigma_{\boldsymbol{\alpha}} = 10$m and $\sigma_{\boldsymbol{\gamma}} = 10$m respectively. As $\sigma_{\boldsymbol{\beta}}$ increases, the CRLB without calibration targets deviates farther and farther away from the case with calibration targets. At a transmitter/receiver location uncertainty level of $\sigma_{\boldsymbol{\beta}} = 100$m which is not rare in practice, the improvement in CRLB from the use of calibration targets is thousands of metres for target position $\mathbf{u}^{\text{o}}$ and tens of metres per second for target velocity $\dot{\mathbf{u}}^{\text{o}}$. This illustrates the significance of using calibration targets to improve the localization accuracy. The CRLB curves versus the calibration target location error level $\sigma_{\boldsymbol{\gamma}}$ are plotted in FIGURE 3(c) where the BR/BRR measurement noise level and the transmitter/receiver location uncertainty level are fixed at $\sigma_{\boldsymbol{\alpha}} = 10$m and $\sigma_{\boldsymbol{\beta}} = 50$m respectively. Interestingly, the trend of CRLB curves implies that, even when the calibration target location error is extremely large, the CRLB with calibration targets are still remarkably below the one without. This justifies again the analysis under (41), and similar results have also been mentioned in previous studies on source localization and sensor network localization issues [16]–[21]. Generally, from FIGURE 3(a), (b) and (c), the use of calibration targets indeed brings a significant improvement in the localization accuracy in the normal case, at least at the CRLB level.

IV. PROPOSED LOCALIZATION ALGORITHM

The potential of calibration targets in improving localization accuracy has been shown in Section III through the analysis of the CRLB. In what follows, so as to fulfill this potential, we will proceed to design a novel closed-form localization algorithm for the aforementioned practical localization scenario. After that, a theoretical analysis will be performed to show that the proposed algorithm achieves the CRLB when satisfying some mild conditions.

A. ALGORITHM DEVELOPMENT

The proposed solution mainly includes two processing steps, referred to as calibration step and localization step respectively. The calibration step is devoted to refine the inaccurate transmitter and receiver locations, and then the localization step is devoted to estimate the target position and velocity.

1) CALIBRATION STEP

To make use of the BR measurements from the calibration targets, the calibration step starts by rearranging (24) as

$$r_{\text{c},k,m,n} - \|\mathbf{c}_k^{\text{o}} - \mathbf{s}_{\text{t},m}^{\text{o}}\| - \|\mathbf{c}_k^{\text{o}} - \mathbf{s}_{\text{r},n}^{\text{o}}\| = \Delta r_{\text{c},k,m,n} \quad (43)$$

Since only the erroneous versions of $\mathbf{c}_k^{\mathrm{o}}$, $\mathbf{s}_{\mathrm{t},m}^{\mathrm{o}}$ and $\mathbf{s}_{\mathrm{r},n}^{\mathrm{o}}$ are available, we plug $\mathbf{c}_k^{\mathrm{o}} = \mathbf{c}_k - \Delta\mathbf{c}_k$, $\mathbf{s}_{\mathrm{t},m}^{\mathrm{o}} = \mathbf{s}_{\mathrm{t},m} - \Delta\mathbf{s}_{\mathrm{t},m}$ and $\mathbf{s}_{\mathrm{r},n}^{\mathrm{o}} = \mathbf{s}_{\mathrm{r},n} - \Delta\mathbf{s}_{\mathrm{r},n}$ into (43), and then expand it around erroneous values $\mathbf{c}_k$, $\mathbf{s}_{\mathrm{t},m}$ and $\mathbf{s}_{\mathrm{r},n}$ to the linear error terms as

$$\begin{aligned} r_{\mathrm{c},k,m,n} - \hat{r}_{\mathrm{c},k,m,n} - \boldsymbol{\rho}_{\mathrm{c},k,\mathrm{t},m}^{\mathrm{T}}\Delta\mathbf{s}_{\mathrm{t},m} - \boldsymbol{\rho}_{\mathrm{c},k,\mathrm{r},n}^{\mathrm{T}}\Delta\mathbf{s}_{\mathrm{r},n} \\ \simeq -(\boldsymbol{\rho}_{\mathrm{c},k,\mathrm{t},m} + \boldsymbol{\rho}_{\mathrm{c},k,\mathrm{r},n})^{\mathrm{T}}\Delta\mathbf{c}_k + \Delta r_{\mathrm{c},k,m,n} \end{aligned} \tag{44}$$

where

$$\hat{r}_{\mathrm{c},k,m,n} = \|\mathbf{c}_k - \mathbf{s}_{\mathrm{t},m}\| + \|\mathbf{c}_k - \mathbf{s}_{\mathrm{r},n}\| \tag{45}$$

$$\boldsymbol{\rho}_{\mathrm{c},k,\mathrm{t},m} = \frac{\mathbf{c}_k - \mathbf{s}_{\mathrm{t},m}}{\|\mathbf{c}_k - \mathbf{s}_{\mathrm{t},m}\|} \tag{46}$$

$$\boldsymbol{\rho}_{\mathrm{c},k,\mathrm{r},n} = \frac{\mathbf{c}_k - \mathbf{s}_{\mathrm{r},n}}{\|\mathbf{c}_k - \mathbf{s}_{\mathrm{r},n}\|} \tag{47}$$

Stacking (44) for all the k, m and n, yields a set of KMN linear equations that can be written in matrix form as

$$\mathbf{h}_{0\mathrm{t}} - \left[\mathbf{G}_{0\mathrm{t}}, \mathbf{O}_{KMN\times 3(M+N)}\right]\Delta\boldsymbol{\beta} = \Delta\mathbf{h}_{0\mathrm{t}} \tag{48}$$

where $\mathbf{h}_{0\mathrm{t}}$ is a KMN-by-1 column vector and $\mathbf{G}_{0\mathrm{t}}$ is a KMN-by-$3(M+N)$ matrix with their elements given by

$$\begin{aligned} [\mathbf{h}_{0\mathrm{t}}]_{(k-1)MN+(m-1)N+n,1} &= r_{\mathrm{c},k,m,n} - \hat{r}_{\mathrm{c},k,m,n}, \\ [\mathbf{G}_{0\mathrm{t}}]_{(k-1)MN+(m-1)N+n,3m-2:3m} &= \boldsymbol{\rho}_{\mathrm{c},k,\mathrm{t},m}^{\mathrm{T}}, \\ [\mathbf{G}_{0\mathrm{t}}]_{(k-1)MN+(m-1)N+n,3M+3n-2:3M+3n} &= \boldsymbol{\rho}_{\mathrm{c},k,\mathrm{r},n}^{\mathrm{T}}, \end{aligned} \tag{49}$$

for $k = 1, 2, \ldots, K$, $m = 1, 2, \ldots, M$, $n = 1, 2, \ldots, N$, and zeros elsewhere. The error vector $\Delta\mathbf{h}_{0\mathrm{t}}$ can be expressed in a compact form as

$$\Delta\mathbf{h}_{0\mathrm{t}} = [\mathbf{C}, \mathbf{O}_{KMN\times 3K}]\Delta\boldsymbol{\gamma} + \Delta\mathbf{r}_{\mathrm{c}} \tag{50}$$

where $\mathbf{C}$ is a KMN-by-$3K$ matrix and its elements are given by $[\mathbf{C}]_{(k-1)MN+(m-1)N+n,3k-2:3k} = -(\boldsymbol{\rho}_{\mathrm{c},k,\mathrm{t},m} + \boldsymbol{\rho}_{\mathrm{c},k,\mathrm{r},n})^{\mathrm{T}}$ for $k = 1, 2, \ldots, K$, $m = 1, 2, \ldots, M$, $n = 1, 2, \ldots, N$, and zeros elsewhere.

To make use of the BRR measurements, we take the derivative of (44) with respect to time as

$$\begin{aligned} \dot{r}_{\mathrm{c},k,m,n} - \hat{\dot{r}}_{\mathrm{c},k,m,n} - \dot{\boldsymbol{\rho}}_{\mathrm{c},k,\mathrm{t},m}^{\mathrm{T}}\Delta\mathbf{s}_{\mathrm{t},m} \\ - \boldsymbol{\rho}_{\mathrm{c},k,\mathrm{t},m}^{\mathrm{T}}\Delta\dot{\mathbf{s}}_{\mathrm{t},m} - \dot{\boldsymbol{\rho}}_{\mathrm{c},k,\mathrm{r},n}^{\mathrm{T}}\Delta\mathbf{s}_{\mathrm{r},n} - \boldsymbol{\rho}_{\mathrm{c},k,\mathrm{r},n}^{\mathrm{T}}\Delta\dot{\mathbf{s}}_{\mathrm{r},n} \\ \simeq -(\dot{\boldsymbol{\rho}}_{\mathrm{c},k,\mathrm{t},m} + \dot{\boldsymbol{\rho}}_{\mathrm{c},k,\mathrm{r},n})^{\mathrm{T}}\Delta\mathbf{c}_k - (\boldsymbol{\rho}_{\mathrm{c},k,\mathrm{t},m} + \boldsymbol{\rho}_{\mathrm{c},k,\mathrm{r},n})^{\mathrm{T}}\Delta\dot{\mathbf{c}}_k \\ + \Delta\dot{r}_{\mathrm{c},k,m,n} \end{aligned} \tag{51}$$

where

$$\hat{\dot{r}}_{\mathrm{c},k,m,n} = \boldsymbol{\rho}_{\mathrm{c},k,\mathrm{t},m}^{\mathrm{T}}(\dot{\mathbf{c}}_k - \dot{\mathbf{s}}_{\mathrm{t},m}) + \boldsymbol{\rho}_{\mathrm{c},k,\mathrm{r},n}^{\mathrm{T}}(\dot{\mathbf{c}}_k - \dot{\mathbf{s}}_{\mathrm{r},n}) \tag{52}$$

$$\dot{\boldsymbol{\rho}}_{\mathrm{c},k,\mathrm{t},m} = \frac{(\dot{\mathbf{c}}_k - \dot{\mathbf{s}}_{\mathrm{t},m}) - \boldsymbol{\rho}_{\mathrm{c},k,\mathrm{t},m}^{\mathrm{T}}(\dot{\mathbf{c}}_k - \dot{\mathbf{s}}_{\mathrm{t},m})\boldsymbol{\rho}_{\mathrm{c},k,\mathrm{t},m}}{\|\mathbf{c}_k - \mathbf{s}_{\mathrm{t},m}\|} \tag{53}$$

$$\dot{\boldsymbol{\rho}}_{\mathrm{c},k,\mathrm{r},n} = \frac{(\dot{\mathbf{c}}_k - \dot{\mathbf{s}}_{\mathrm{r},n}) - \boldsymbol{\rho}_{\mathrm{c},k,\mathrm{r},n}^{\mathrm{T}}(\dot{\mathbf{c}}_k - \dot{\mathbf{s}}_{\mathrm{r},n})\boldsymbol{\rho}_{\mathrm{c},k,\mathrm{r},n}}{\|\mathbf{c}_k - \mathbf{s}_{\mathrm{r},n}\|} \tag{54}$$

Collecting (51) for all the k, m and n, produces a set of KMN linear equations that can be arranged in matrix form as

$$\mathbf{h}_{0\mathrm{f}} - [\mathbf{G}_{0\mathrm{f}}, \mathbf{G}_{0\mathrm{t}}]\Delta\boldsymbol{\beta} = \Delta\mathbf{h}_{0\mathrm{f}} \tag{55}$$

where $\mathbf{h}_{0\mathrm{f}}$ is a KMN-by-1 column vector, $\mathbf{G}_{0\mathrm{f}}$ is a KMN-by-$6(M+N)$ matrix, and their elements are given by

$$\begin{aligned} [\mathbf{h}_{0\mathrm{f}}]_{(k-1)MN+(m-1)N+n,1} &= \dot{r}_{\mathrm{c},k,m,n} - \hat{\dot{r}}_{\mathrm{c},k,m,n}, \\ [\mathbf{G}_{0\mathrm{f}}]_{(k-1)MN+(m-1)N+n,3m-2:3m} &= \dot{\boldsymbol{\rho}}_{\mathrm{c},k,\mathrm{t},m}^{\mathrm{T}}, \\ [\mathbf{G}_{0\mathrm{f}}]_{(k-1)MN+(m-1)N+n,3M+3n-2:3M+3n} &= \dot{\boldsymbol{\rho}}_{\mathrm{c},k,\mathrm{r},n}^{\mathrm{T}}, \end{aligned} \tag{56}$$

for $k = 1, 2, \ldots, K$, $m = 1, 2, \ldots, M$, $n = 1, 2, \ldots, N$, and zeros elsewhere. Furthermore, error vector $\Delta\mathbf{h}_{0\mathrm{f}}$ can be expressed in a compact form as

$$\Delta\mathbf{h}_{0\mathrm{f}} = [\dot{\mathbf{C}}, \mathbf{C}]\Delta\boldsymbol{\gamma} + \Delta\dot{\mathbf{r}}_{\mathrm{c}} \tag{57}$$

where $\dot{\mathbf{C}}$ is aKMN-by-$3K$ matrix with its elements given by $[\dot{\mathbf{C}}]_{(k-1)MN+(m-1)N+n,3k-2:3k} = -(\dot{\boldsymbol{\rho}}_{\mathrm{c},k,\mathrm{t},m} + \dot{\boldsymbol{\rho}}_{\mathrm{c},k,\mathrm{r},n})^{\mathrm{T}}$ for $k = 1, 2, \ldots, K$, $m = 1, 2, \ldots, M$, $n = 1, 2, \ldots, N$, and zeros elsewhere.

Putting the two sets of equations in (50) and (57) together, yields the total equation set as

$$\mathbf{h}_0 - \mathbf{G}_0\Delta\boldsymbol{\beta} = \Delta\mathbf{h}_0 \tag{58}$$

where

$$\mathbf{h}_0 = \begin{bmatrix} \mathbf{h}_{0\mathrm{t}} \\ \mathbf{h}_{0\mathrm{f}} \end{bmatrix}, \quad \mathbf{G}_0 = \begin{bmatrix} \mathbf{G}_{0\mathrm{t}} & \mathbf{O}_{KMN\times 3(M+N)} \\ \mathbf{G}_{0\mathrm{f}} & \mathbf{G}_{0\mathrm{t}} \end{bmatrix} \tag{59}$$

The error vector $\Delta\mathbf{h}_0$ is given by

$$\begin{aligned} \Delta\mathbf{h}_0 &= \begin{bmatrix} \mathbf{C} & \mathbf{O}_{KMN\times 3K} \\ \dot{\mathbf{C}} & \mathbf{C} \end{bmatrix}\Delta\boldsymbol{\gamma} + \begin{bmatrix} \Delta\dot{\mathbf{r}}_{\mathrm{c}} \\ \Delta\dot{\mathbf{r}}_{\mathrm{c}} \end{bmatrix} \\ &= \mathbf{C}_1\Delta\boldsymbol{\gamma} + \Delta\boldsymbol{\alpha}_{\mathrm{c}} \end{aligned} \tag{60}$$

In (58), $\Delta\boldsymbol{\beta}$ reflects the difference between the true transmitter/receiver locations and the erroneous versions. In order to refine the transmitter and receiver locations, $\Delta\boldsymbol{\beta}$ shall be estimated as accurately as possible. Recall that $\Delta\boldsymbol{\beta}$ is a zero-mean Gaussian distributed random vector with covariance matrix $\mathbf{Q}_{\boldsymbol{\beta}}$. According to the Bayesian Gauss-Markov theorem [25], the linear minimum mean square error (LMMSE) estimator for the given model in (58) is

$$\begin{aligned} \Delta\hat{\boldsymbol{\beta}} = \left(\mathbf{Q}_{\boldsymbol{\beta}}^{-1} + \mathbf{G}_0^{\mathrm{T}}(\mathbf{C}_1\mathbf{Q}_{\boldsymbol{\gamma}}\mathbf{C}_1^{\mathrm{T}} + \mathbf{Q}_{\boldsymbol{\alpha}\mathrm{c}})^{-1}\mathbf{G}_0\right)^{-1} \\ \times \mathbf{G}_0^{\mathrm{T}}(\mathbf{C}_1\mathbf{Q}_{\boldsymbol{\gamma}}\mathbf{C}_1^{\mathrm{T}} + \mathbf{Q}_{\boldsymbol{\alpha}\mathrm{c}})^{-1}\mathbf{h}_0 \end{aligned} \tag{61}$$

From Bayesian Gauss-Markov theorem [25], in order to perfectly determine $\Delta\boldsymbol{\beta}$ and completely remove the transmitter/receiver location uncertainties, the number of transmitters, receivers and calibration targets should satisfy $MNK \geq 3(M+N)$ (meanwhile the calibration BR/BRR measurements and the calibration target locations are noise free, i.e. $\mathbf{Q}_{\boldsymbol{\alpha}\mathrm{c}}$ and $\mathbf{Q}_{\boldsymbol{\gamma}}$ tends to zero). However, we don't have to completely remove the transmitter/receiver location errors. When the number of transmitters, receivers and calibration targets does not satisfy $MNK \geq 3(M+N)$ (and the calibration BR/BRR measurements and the calibration targets are noisy), the transmitter/receiver location error vector $\Delta\boldsymbol{\beta}$ can still be estimated approximately and the transmitter/receiver location uncertainties can be partially removed. This is reflected

in the formula of LMMSE estimator given in (61), where $(\mathbf{Q}_{\boldsymbol{\beta}}^{-1} + \mathbf{G}_0^{\mathrm{T}}(\mathbf{C}_1\mathbf{Q}_{\boldsymbol{\gamma}}\mathbf{C}_1^{\mathrm{T}} + \mathbf{Q}_{\boldsymbol{\alpha}\mathrm{c}})^{-1}\mathbf{G}_0)$ is invertible and $\Delta\boldsymbol{\beta}$ can be estimated to partially calibrate the inaccurate transmitter/receiver locations even when there is only $K = 1$ calibration target. That is to say, the calibration step has no additional request on the number of transmitters, receivers and calibration targets.

Under the assumption that the noise in $\mathbf{C}_1$ and $\mathbf{G}_0$ is sufficiently small to be ignored, the covariance matrix of $\Delta\hat{\boldsymbol{\beta}}$ can be approximated by

$$\mathrm{cov}(\Delta\boldsymbol{\beta}-\Delta\hat{\boldsymbol{\beta}})=\left(\mathbf{Q}_{\boldsymbol{\beta}}^{-1}+\mathbf{G}_0^{\mathrm{T}}(\mathbf{C}_1\mathbf{Q}_{\boldsymbol{\gamma}}\mathbf{C}_1^{\mathrm{T}}+\mathbf{Q}_{\boldsymbol{\alpha}\mathrm{c}})^{-1}\mathbf{G}_0\right)^{-1} \quad (62)$$

Using the estimate of $\Delta\boldsymbol{\beta}$ in (61), we can refine the transmitter and receiver locations as

$$\hat{\boldsymbol{\beta}} = \boldsymbol{\beta} - \Delta\hat{\boldsymbol{\beta}} \quad (63)$$

Utilizing the fact $\boldsymbol{\beta} = \boldsymbol{\beta}^{\mathrm{o}} + \Delta\boldsymbol{\beta}$, we can rewrite $\hat{\boldsymbol{\beta}}$ in (63) as $\hat{\boldsymbol{\beta}} = \boldsymbol{\beta}^{\mathrm{o}} + \Delta\boldsymbol{\beta} - \Delta\hat{\boldsymbol{\beta}}$. Hence, the refined estimate of transmitter/receiver locations $\hat{\boldsymbol{\beta}}$ has a covariance matrix identical with (62). Forming the inverse of $\mathrm{cov}(\Delta\boldsymbol{\beta} - \Delta\hat{\boldsymbol{\beta}})$ and then comparing it with $\mathbf{Q}_{\boldsymbol{\beta}}^{-1}$, we have $\mathrm{cov}(\Delta\boldsymbol{\beta} - \Delta\hat{\boldsymbol{\beta}})^{-1} - \mathbf{Q}_{\boldsymbol{\beta}}^{-1} = \mathbf{G}_0^{\mathrm{T}}(\mathbf{C}_1\mathbf{Q}_{\boldsymbol{\gamma}}\mathbf{C}_1^{\mathrm{T}} + \mathbf{Q}_{\boldsymbol{\alpha}\mathrm{c}})^{-1}\mathbf{G}_0$. Because $\mathbf{G}_0^{\mathrm{T}}(\mathbf{C}_1\mathbf{Q}_{\boldsymbol{\gamma}}\mathbf{C}_1^{\mathrm{T}} + \mathbf{Q}_{\boldsymbol{\alpha}\mathrm{c}})^{-1}\mathbf{G}_0$ has a symmetric structure and $\mathbf{G}_0$ is not full column rank, we infer that $\mathrm{cov}(\Delta\boldsymbol{\beta} - \Delta\hat{\boldsymbol{\beta}})^{-1} \geq \mathbf{Q}_{\boldsymbol{\beta}}^{-1}$. According to the PSD matrix property [24], $\mathrm{cov}(\Delta\boldsymbol{\beta} - \Delta\hat{\boldsymbol{\beta}})^{-1} \geq \mathbf{Q}_{\boldsymbol{\beta}}^{-1}$ is equivalent to $\mathbf{Q}_{\boldsymbol{\beta}} \geq \mathrm{cov}(\Delta\boldsymbol{\beta} - \Delta\hat{\boldsymbol{\beta}})$. That is, the refined transmitter and receiver locations perform leastwise as well as, if not better than, the original ones, in terms of target localization accuracy.

2) LOCALIZATION STEP

In the localization step, the refined transmitter and receiver locations from the calibration step and the BR/BRR measurements from the unknown target will be employed to determine the target position $\mathbf{u}^{\mathrm{o}}$ and velocity $\dot{\mathbf{u}}^{\mathrm{o}}$. The processing in this step is basically the same as that in [15], expect that the transmitter and receiver location vector and the corresponding covariance matrix are replaced by $\hat{\boldsymbol{\beta}}$ and $\mathrm{cov}(\hat{\boldsymbol{\beta}} - \Delta\hat{\boldsymbol{\beta}})$ respectively. For completeness, the basic processing involved in this stage is briefly presented below, and the readers are referred to [15] for further details.

By defining the auxiliary vector

$$\boldsymbol{\eta}^{\mathrm{o}}=\left[(\mathbf{u}^{\mathrm{o}})^{\mathrm{T}},R_{\mathrm{t},1}^{\mathrm{o}},R_{\mathrm{t},2}^{\mathrm{o}},\ldots,R_{\mathrm{t},M}^{\mathrm{o}},(\dot{\mathbf{u}}^{\mathrm{o}})^{\mathrm{T}},\dot{R}_{\mathrm{t},1}^{\mathrm{o}},\dot{R}_{\mathrm{t},2}^{\mathrm{o}},\ldots,\dot{R}_{\mathrm{t},M}^{\mathrm{o}}\right]^{\mathrm{T}} \quad (64)$$

where $R_{\mathrm{t},1}^{\mathrm{o}}, R_{\mathrm{t},2}^{\mathrm{o}}, \ldots, R_{\mathrm{t},M}^{\mathrm{o}}, \dot{R}_{\mathrm{t},1}^{\mathrm{o}}, \dot{R}_{\mathrm{t},2}^{\mathrm{o}}, \ldots, \dot{R}_{\mathrm{t},M}^{\mathrm{o}}$ are the introduced auxiliary parameters, a pseudolinear set equations is established from the nonlinear BR and BRR measurement equations with respect to the unknown target,

$$\mathbf{G}_1\boldsymbol{\eta}^{\mathrm{o}} = \mathbf{h}_1 + \Delta\mathbf{h}_1 \quad (65)$$

where $\mathbf{G}_1$ is a $2MN$-by-$2(M+3)$ matrix, $\mathbf{h}_1$ is a $2MN$-by-1 column vector, and their elements are

$$\begin{aligned}
[\mathbf{G}_1]_{(m-1)N+n,1:3} &= (\hat{\mathbf{s}}_{\mathrm{t},m} - \hat{\mathbf{s}}_{\mathrm{r},n})^{\mathrm{T}},\\
[\mathbf{G}_1]_{(m-1)N+n,m+3} &= r_{m,n},\\
[\mathbf{G}_1]_{MN+(m-1)N+n,1:3} &= (\hat{\dot{s}}_{\mathrm{t},m} - \hat{\dot{s}}_{\mathrm{r},n})^{\mathrm{T}},\\
[\mathbf{G}_1]_{MN+(m-1)N+n,m+3} &= \dot{r}_{m,n}\\
[\mathbf{G}_1]_{MN+(m-1)N+n,M+4:M+6} &= (\hat{\mathbf{s}}_{\mathrm{t},m} - \hat{\mathbf{s}}_{\mathrm{r},n})^{\mathrm{T}},\\
[\mathbf{G}_1]_{MN+(m-1)N+n,M+6+m} &= r_{m,n}\\
[\mathbf{h}_1]_{(m-1)N+n,1} &= r_{m,n}^2 + \hat{\mathbf{s}}_{\mathrm{t},m}^{\mathrm{T}}\hat{\mathbf{s}}_{\mathrm{t},m} - \hat{\mathbf{s}}_{\mathrm{r},n}^{\mathrm{T}}\hat{\mathbf{s}}_{\mathrm{r},n},\\
[\mathbf{h}_1]_{MN+(m-1)N+n,1} &= 2(r_{m,2}\dot{r}_{m,2} + \hat{\mathbf{s}}_{\mathrm{t},m}^{\mathrm{T}}\hat{\dot{\mathbf{s}}}_{\mathrm{t},m}\\
&\quad -\hat{\mathbf{s}}_{\mathrm{r},2}^{\mathrm{T}}\hat{\dot{\mathbf{s}}}_{\mathrm{r},2}),
\end{aligned} \quad (66)$$

for $m = 1, 2, \ldots, M$, $n = 1, 2, \ldots, N$, and zeros elsewhere.

On the right side of (65), the error vector $\Delta\mathbf{h}_1$ is defined as

$$\Delta\mathbf{h}_1 = \mathbf{B}_1\Delta\boldsymbol{\alpha} + \mathbf{D}_1\Delta\boldsymbol{\beta} \quad (67)$$

where

$$\mathbf{B}_1=\begin{bmatrix}\mathbf{B} & \mathbf{O}_{MN\times MN}\\ \dot{\mathbf{B}} & \mathbf{B}\end{bmatrix},\quad \mathbf{D}_1=\begin{bmatrix}\mathbf{D} & \mathbf{O}_{MN\times 3(M+N)}\\ \dot{\mathbf{D}} & \mathbf{D}\end{bmatrix} \quad (68)$$

with the elements of blocks $\mathbf{B}$, $\dot{\mathbf{B}}$, $\mathbf{D}$ and $\dot{\mathbf{D}}$ given by

$$\begin{aligned}
[\mathbf{B}]_{(m-1)N+n,(m-1)N+n} &= -2R_{\mathrm{r},n}^{\mathrm{o}},\\
[\dot{\mathbf{B}}]_{MN+(m-1)N+n,(m-1)N+n} &= -2\dot{R}_{\mathrm{r},n}^{\mathrm{o}},\\
[\mathbf{D}]_{(m-1)N+n,3m-2:3m} &= 2(\mathbf{u}^{\mathrm{o}} - \hat{\mathbf{s}}_{\mathrm{t},m})^{\mathrm{T}},\\
[\mathbf{D}]_{(m-1)N+n,3M+3n-2:3M+3n} &= -2(\mathbf{u}^{\mathrm{o}} - \hat{\mathbf{s}}_{\mathrm{r},1})^{\mathrm{T}},\\
[\dot{\mathbf{D}}]_{(m-1)N+n,3m-2:3m} &= 2(\dot{u}^{\mathrm{o}} - \hat{\dot{\mathbf{s}}}_{\mathrm{t},m})^{\mathrm{T}},\\
[\dot{\mathbf{D}}]_{(m-1)N+n,3M+3n-2:3M+3n} &= -2(\dot{\mathbf{u}}^{\mathrm{o}} - \hat{\dot{\mathbf{s}}}_{\mathrm{r},1})^{\mathrm{T}},
\end{aligned} \quad (69)$$

for $m = 1, 2, \ldots, M$, $n = 1, 2, \ldots, N$, and zeros elsewhere.

From (65), $\boldsymbol{\eta}^{\mathrm{o}}$ is estimated by the WLS minimization as

$$\boldsymbol{\eta} = (\mathbf{G}_1^{\mathrm{T}}\mathbf{W}_1\mathbf{G}_1)^{-1}\mathbf{G}_1^{\mathrm{T}}\mathbf{W}_1\mathbf{h}_1 \quad (70)$$

where $\mathbf{W}_1$ is the weighting matrix computed by

$$\mathbf{W}_1 = \left[\mathbf{B}_1\mathbf{Q}_{\boldsymbol{\alpha}}\mathbf{B}_1^{\mathrm{T}} + \mathbf{D}_1\mathrm{cov}(\hat{\boldsymbol{\beta}} - \Delta\hat{\boldsymbol{\beta}})\mathbf{D}_1^{\mathrm{T}}\right]^{-1} \quad (71)$$

Under the condition that the measurement noise and the transmitter/receiver location error are sufficiently small, the covariance matrix of $\boldsymbol{\eta}$ is given by

$$\mathrm{cov}(\boldsymbol{\eta}) = (\mathbf{G}_1^{\mathrm{T}}\mathbf{W}_1\mathbf{G}_1)^{-1} \quad (72)$$

Denote the estimated values of $\mathbf{u}^{\mathrm{o}}, R_{\mathrm{t},1}^{\mathrm{o}}, R_{\mathrm{t},2}^{\mathrm{o}}, \ldots, R_{\mathrm{t},M}^{\mathrm{o}}, \dot{\mathbf{u}}^{\mathrm{o}}, \dot{R}_{\mathrm{t},1}^{\mathrm{o}}, \dot{R}_{\mathrm{t},2}^{\mathrm{o}}, \ldots, \dot{R}_{\mathrm{t},M}^{\mathrm{o}}$ contained in $\boldsymbol{\eta}$ by $\mathbf{u}, R_{\mathrm{t},1}, R_{\mathrm{t},2}, \ldots, R_{\mathrm{t},M}, \dot{\mathbf{u}}, \dot{R}_{\mathrm{t},1}, \dot{R}_{\mathrm{t},2}, \ldots, \dot{R}_{\mathrm{t},M}$ respectively. By exploiting the functional relationship between the auxiliary parameters and the target location parameters, another set of linear equation is established as

$$\mathbf{G}_2\boldsymbol{\theta}^{\mathrm{o}} = \mathbf{h}_2 + \Delta\mathbf{h}_2 \quad (73)$$

where $\boldsymbol{\theta}^{\mathrm{o}} = [(\mathbf{u}^{\mathrm{o}})^{\mathrm{T}}, (\dot{\mathbf{u}}^{\mathrm{o}})^{\mathrm{T}}]^{\mathrm{T}}$, $\mathbf{G}_2$ is a $2(M+3)$-by-6 matrix, $\mathbf{h}_2$ is a $2(M+3)$-by-1 column vector. The elements

of $\mathbf{G}_2$ and $\mathbf{h}_2$ are

$$\begin{aligned}
[\mathbf{G}_2]_{1:3,1:3} &= \mathbf{I}_3, \quad [\mathbf{G}_2]_{m+3,1:3} = 2\hat{\mathbf{s}}_{\mathrm{t},m}^{\mathrm{T}}, \\
[\mathbf{G}_2]_{M+4:M+6,4:6} &= \mathbf{I}_3, \quad [\mathbf{G}_2]_{M+6+m,1:3} = 2\dot{\hat{\mathbf{s}}}_{\mathrm{t},m}^{\mathrm{T}}, \\
[\mathbf{G}_2]_{M+6+m,4:6} &= 2\hat{\mathbf{s}}_{\mathrm{t},m}^{\mathrm{T}}, \quad [\mathbf{h}_2]_{1:3,1} = \mathbf{u}, \\
[\mathbf{h}_2]_{m+3,1} &= \mathbf{u}^{\mathrm{T}}\mathbf{u} - R_{\mathrm{t},m}^2 + \hat{\mathbf{s}}_{\mathrm{t},m}^{\mathrm{T}}\hat{\mathbf{s}}_{\mathrm{t},m}, \\
[\mathbf{h}_2]_{M+4:M+6,1} &= \dot{\mathbf{u}}, \\
[\mathbf{h}_2]_{M+6+m,1} &= 2\mathbf{u}^{\mathrm{T}}\dot{\mathbf{u}} - 2R_{\mathrm{t},m}\dot{R}_{\mathrm{t},m} + \hat{\mathbf{s}}_{\mathrm{t},m}^{\mathrm{T}}\dot{\hat{\mathbf{s}}}_{\mathrm{t},m}
\end{aligned} \tag{74}$$

The error vector $\Delta\mathbf{h}_2$ is defined as

$$\Delta\mathbf{h}_2 = \mathbf{B}_2\Delta\boldsymbol{\eta} + \mathbf{D}_2\Delta\boldsymbol{\beta} \tag{75}$$

where

$$\begin{aligned}
\mathbf{B}_2 &= \begin{bmatrix} \tilde{B} & \mathbf{O}_{(M+3)\times(M+3)} \\ \dot{\tilde{\mathbf{B}}} & \tilde{\mathbf{B}} \end{bmatrix}, \\
\mathbf{D}_2 &= \begin{bmatrix} \tilde{\mathbf{D}} & \mathbf{O}_{(M+3)\times 2(M+N)} \\ \dot{\tilde{\mathbf{D}}} & \tilde{\mathbf{D}} \end{bmatrix}
\end{aligned} \tag{76}$$

with the elements of blocks $\tilde{\mathbf{B}}$, $\dot{\tilde{B}}$, $\tilde{\mathbf{D}}$ and $\dot{\tilde{D}}$ given by

$$\begin{aligned}
[\tilde{\mathbf{B}}]_{1:3,1:3} &= -\mathbf{I}_3, \quad [\tilde{\mathbf{B}}]_{m+3,1:3} = -2\mathbf{u}^{\mathrm{T}}, \\
[\tilde{\mathbf{B}}]_{m+3,m+3} &= 2R_{\mathrm{t},m}, \quad [\dot{\tilde{\mathbf{B}}}]_{m+3,1:3} = -2\dot{\mathbf{u}}^{\mathrm{T}}, \\
[\dot{\tilde{\mathbf{B}}}]_{m+3,m+3} &= 2\dot{R}_{\mathrm{t},m}, \\
[\tilde{D}]_{m+3,3m-2:3m} &= 2(\mathbf{u}^{\mathrm{o}} - \mathbf{s}_{\mathrm{t},m})^{\mathrm{T}}, \\
[\dot{\tilde{\mathbf{D}}}]_{m+3,3m-2:3m} &= 2(\dot{\mathbf{u}}^{\mathrm{o}} - \dot{\mathbf{s}}_{\mathrm{t},m})^{\mathrm{T}}
\end{aligned} \tag{77}$$

for $m = 1, 2, \ldots, M$, $n = 1, 2, \ldots, N$, and zeros elsewhere.

From (73), $\boldsymbol{\theta}^{\mathrm{o}}$ is determined by using the WLS minimization as

$$\boldsymbol{\theta} = (\mathbf{G}_2^{\mathrm{T}}\mathbf{W}_2\mathbf{G}_2)^{-1}\mathbf{G}_2^{\mathrm{T}}\mathbf{W}_2\mathbf{h}_2 \tag{78}$$

where $\mathbf{W}_2$ is the weighting matrix computed by

$$\begin{aligned}
\mathbf{W}_2 = \Big[&\mathbf{B}_2\mathrm{cov}(\boldsymbol{\eta})\mathbf{B}_2^{\mathrm{T}} + \mathbf{D}_2\mathrm{cov}(\hat{\boldsymbol{\beta}} - \Delta\hat{\boldsymbol{\beta}})\mathbf{D}_2^{\mathrm{T}} \\
&+ \mathbf{B}_2(\mathbf{G}_1^{\mathrm{T}}\mathbf{W}_1\mathbf{G}_1)^{-1}\mathbf{G}_1^{\mathrm{T}}\mathbf{W}_1\mathbf{D}_1\mathrm{cov}(\hat{\boldsymbol{\beta}} - \Delta\hat{\boldsymbol{\beta}})\mathbf{D}_2^{\mathrm{T}} \\
&+ \mathbf{D}_2\mathrm{cov}(\hat{\boldsymbol{\beta}} - \Delta\hat{\boldsymbol{\beta}})\mathbf{D}_1^{\mathrm{T}}\mathbf{W}_1\mathbf{G}_1(\mathbf{G}_1^{\mathrm{T}}\mathbf{W}_1\mathbf{G}_1)^{-1}\mathbf{B}_2^{\mathrm{T}}\Big]^{-1}
\end{aligned} \tag{79}$$

Given sufficiently small measurement noise and transmitter/receiver location error, the covariance matrix of $\boldsymbol{\theta}$ is given by

$$\mathrm{cov}(\boldsymbol{\theta}) = (\mathbf{G}_2^{\mathrm{T}}\mathbf{W}_2\mathbf{G}_2)^{-1} \tag{80}$$

In the localization step, we employ MN BR measurements and MN BRR measurements, produced from the M transmitters and N receivers, to determine the unknown target location vector $\boldsymbol{\theta}^{\mathrm{o}}$. In theory, to obtain a unique estimate of the unknown target location, the number of transmitters and receivers should satisfy $MN \geq 3$. However, for the two-step weighted least squares localization method employed in the localization step, we introduced $2M$ auxiliary parameters $R_{\mathrm{t},1}^{\mathrm{o}}, R_{\mathrm{t},2}^{\mathrm{o}}, \ldots, R_{\mathrm{t},M}^{\mathrm{o}}, \dot{R}_{\mathrm{t},1}^{\mathrm{o}}, \dot{R}_{\mathrm{t},2}^{\mathrm{o}}, \ldots, \dot{R}_{\mathrm{t},M}^{\mathrm{o}}$ to construct an auxiliary vector $\boldsymbol{\eta}^{\mathrm{o}}$ in (65). Hence, in order to avoid underdetermined problem, the number of transmitters and receivers should satisfy $MN \geq M + 3$. If we introduce $R_{\mathrm{r},1}^{\mathrm{o}}, R_{\mathrm{r},2}^{\mathrm{o}}, \ldots, R_{\mathrm{r},N}^{\mathrm{o}}, \dot{R}_{\mathrm{r},1}^{\mathrm{o}}, \dot{R}_{\mathrm{r},2}^{\mathrm{o}}, \ldots, \dot{R}_{\mathrm{r},N}^{\mathrm{o}}$ as auxiliary parameters, the number of transmitters and receivers should satisfy $MN \geq N + 3$.

B. PERFORMANCE ANALYSIS

As mentioned before, the CRLB traces out a lower bound for minimum possible variance that an unbiased estimator can achieve. In this subsection, we shall analyze the efficiency of the proposed solution by comparing its covariance matrix with the CRLB. For easier derivation, we would compare their inverse, rather than directly compare themselves. The CRLB has been presented in (39). Invoke the matrix inversion lemma [23] to (39) and employ the definitions of $\mathbf{X}$ and $\mathbf{Y}$, then we have after mathematical simplifications,

$$\begin{aligned}
\mathbf{CRLB}_{\mathrm{c}}(\boldsymbol{\theta}^{\mathrm{o}})^{-1} = &\left(\frac{\partial\boldsymbol{\alpha}^{\mathrm{o}}}{\partial\boldsymbol{\theta}^{\mathrm{o}}}\right)^{\mathrm{T}}\mathbf{Q}_{\boldsymbol{\alpha}}^{-1}\left(\frac{\partial\boldsymbol{\alpha}^{\mathrm{o}}}{\partial\boldsymbol{\theta}^{\mathrm{o}}}\right) \\
&- \left(\frac{\partial\boldsymbol{\alpha}^{\mathrm{o}}}{\partial\boldsymbol{\theta}^{\mathrm{o}}}\right)^{\mathrm{T}}\mathbf{Q}_{\boldsymbol{\alpha}}^{-1}\left(\frac{\partial\boldsymbol{\alpha}^{\mathrm{o}}}{\partial\boldsymbol{\beta}^{\mathrm{o}}}\right)\breve{\mathbf{Z}}^{-1}\left(\frac{\partial\boldsymbol{\alpha}^{\mathrm{o}}}{\partial\boldsymbol{\beta}^{\mathrm{o}}}\right)^{\mathrm{T}} \\
&\times\mathbf{Q}_{\boldsymbol{\alpha}}^{-1}\left(\frac{\partial\boldsymbol{\alpha}^{\mathrm{o}}}{\partial\boldsymbol{\theta}^{\mathrm{o}}}\right)
\end{aligned} \tag{81}$$

where the definition of $\breve{\mathbf{Z}}$ has been given in (38).

On the other hand, by substituting (79), (72), (71) and (62) into (80) successively, we can express the inverse of $\mathrm{cov}(\boldsymbol{\theta})$ as

$$\mathrm{cov}(\boldsymbol{\theta})^{-1} = \mathbf{G}_3^{\mathrm{T}}\mathbf{Q}_{\boldsymbol{\alpha}}^{-1}\mathbf{G}_3 - \mathbf{G}_3^{\mathrm{T}}\mathbf{Q}_{\boldsymbol{\alpha}}^{-1}\mathbf{G}_4\bar{\mathbf{Z}}^{-1}\mathbf{G}_4^{\mathrm{T}}\mathbf{Q}_{\boldsymbol{\alpha}}^{-1}\mathbf{G}_3 \tag{82}$$

in which $\mathbf{G}_3 = \mathbf{B}_1^{-1}\mathbf{G}_1\mathbf{B}_2^{-1}\mathbf{G}_2$, $\mathbf{G}_4 = \mathbf{B}_1^{-1}\mathbf{D}_1$, and $\bar{\mathbf{Z}} = \mathbf{Q}_{\boldsymbol{\beta}}^{-1} + \mathbf{G}_4^{\mathrm{T}}\mathbf{Q}_{\boldsymbol{\alpha}}^{-1}\mathbf{G}_4 + \mathbf{G}_0^{\mathrm{T}}(\mathbf{C}_1\mathbf{Q}_{\boldsymbol{\gamma}}\mathbf{C}_1^{\mathrm{T}} + \mathbf{Q}_{\boldsymbol{\alpha}\mathrm{c}})^{-1}\mathbf{G}_0$.

Comparing (81) with (82), we observe that $\mathbf{CRLB}_{\mathrm{c}}(\boldsymbol{\theta}^{\mathrm{o}})^{-1}$ and $\mathrm{cov}(\boldsymbol{\theta})^{-1}$ are identical in structure. Next, we proceed to prove their equivalency under the following two sets of conditions:

C1) $\|\Delta\mathbf{s}_{\mathrm{t},m}\|/\|\mathbf{c}_k^{\mathrm{o}} - \mathbf{s}_{\mathrm{t},m}^{\mathrm{o}}\| \simeq 0$, $\|\Delta\dot{\mathbf{s}}_{\mathrm{t},m}\|/\|\dot{\mathbf{c}}_k^{\mathrm{o}} - \dot{\mathbf{s}}_{\mathrm{t},m}^{\mathrm{o}}\| \simeq 0$, $\|\Delta\mathbf{s}_{\mathrm{r},n}\|/\|\mathbf{c}_k^{\mathrm{o}} - \mathbf{s}_{\mathrm{r},n}^{\mathrm{o}}\| \simeq 0$, $\|\Delta\dot{\mathbf{s}}_{\mathrm{r},n}\|/\|\dot{\mathbf{c}}_k^{\mathrm{o}} - \dot{\mathbf{s}}_{\mathrm{r},n}^{\mathrm{o}}\| \simeq 0$, $\|\Delta\mathbf{c}_k\|/\|\mathbf{c}_k^{\mathrm{o}} - \mathbf{s}_{\mathrm{t},m}^{\mathrm{o}}\| \simeq 0$, $\|\Delta\dot{\mathbf{c}}_k\|/\|\dot{\mathbf{c}}_k^{\mathrm{o}} - \dot{\mathbf{s}}_{\mathrm{t},m}^{\mathrm{o}}\| \simeq 0$, $\|\Delta\mathbf{c}_k\|/\|\mathbf{c}_k^{\mathrm{o}} - \mathbf{s}_{\mathrm{r},n}^{\mathrm{o}}\| \simeq 0$, $\|\Delta\dot{\mathbf{c}}_k\|/\|\dot{\mathbf{c}}_k^{\mathrm{o}} - \dot{\mathbf{s}}_{\mathrm{r},n}^{\mathrm{o}}\| \simeq 0$, for $k = 1, 2, \ldots, K$, $m = 1, 2, \ldots, M$, $n = 1, 2, \ldots, N$;

C2) $\|\Delta r_{m,n}\|/\|\mathbf{u}^{\mathrm{o}} - \mathbf{s}_{\mathrm{t},m}^{\mathrm{o}}\| \simeq 0$, $\|\Delta\dot{r}_{m,n}\|/\|\dot{\mathbf{u}}^{\mathrm{o}} - \dot{\mathbf{s}}_{\mathrm{t},m}^{\mathrm{o}}\| \simeq 0$, $\|\Delta r_{m,n}\|/\|\mathbf{u}^{\mathrm{o}} - \mathbf{s}_{\mathrm{r},n}^{\mathrm{o}}\| \simeq 0$, $\|\Delta\dot{r}_{m,n}\|/\|\dot{\mathbf{u}}^{\mathrm{o}} - \dot{\mathbf{s}}_{\mathrm{r},n}^{\mathrm{o}}\| \simeq 0$, $\|\Delta\mathbf{s}_{\mathrm{t},m} - \Delta\hat{\mathbf{s}}_{\mathrm{t},m}\|/\|\mathbf{u}^{\mathrm{o}} - \mathbf{s}_{\mathrm{t},m}^{\mathrm{o}}\|\|\mathbf{u}^{\mathrm{o}} - \mathbf{s}_{\mathrm{t},m}^{\mathrm{o}}\| \simeq 0$, $\|\Delta\dot{\mathbf{s}}_{\mathrm{t},m} - \Delta\dot{\hat{\mathbf{s}}}_{\mathrm{t},m}\|/\|\dot{\mathbf{u}}^{\mathrm{o}} - \dot{\mathbf{s}}_{\mathrm{t},m}^{\mathrm{o}}\| \simeq 0$, $\|\Delta\mathbf{s}_{\mathrm{r},n} - \Delta\hat{\mathbf{s}}_{\mathrm{r},n}\|/\|\mathbf{u}^{\mathrm{o}} - \mathbf{s}_{\mathrm{r},n}^{\mathrm{o}}\| \simeq 0$, $\|\Delta\dot{\mathbf{s}}_{\mathrm{r},n} - \Delta\dot{\hat{\mathbf{s}}}_{\mathrm{r},n}\|/\|\dot{\mathbf{u}}^{\mathrm{o}} - \dot{\mathbf{s}}_{\mathrm{r},n}^{\mathrm{o}}\| \simeq 0$, for $m = 1, 2, \ldots, M$, $n = 1, 2, \ldots, N$.

The set of conditions C1 implies the transmitter/receiver location error and the calibration target location error are negligibly small compared with the range and range rate between the calibration target and the transmitter/receiver. The set of conditions C2 implies the BR/BRR measurement noise and the error in the refined transmitter/receiver locations

are negligibly small compared to the range and range rate between the target and the transmitter/receiver. Using the conditions in C1 and C2, we obtain, after some involved algebraic manipulations, that

$$\mathbf{G}_3 \simeq \frac{\partial \boldsymbol{\alpha}^{\mathrm{o}}}{\partial \boldsymbol{\theta}^{\mathrm{o}}}, \quad \mathbf{G}_4 \simeq -\frac{\partial \boldsymbol{\alpha}^{\mathrm{o}}}{\partial \boldsymbol{\beta}^{\mathrm{o}}},$$
$$\mathbf{G}_0 \simeq -\frac{\partial \boldsymbol{\alpha}_{\mathrm{c}}^{\mathrm{o}}}{\partial \boldsymbol{\beta}^{\mathrm{o}}}, \quad \mathbf{C}_1 \simeq -\frac{\partial \boldsymbol{\alpha}_{\mathrm{c}}^{\mathrm{o}}}{\partial \boldsymbol{\gamma}^{\mathrm{o}}} \tag{83}$$

Based on this, we can deduce $\mathrm{cov}(\boldsymbol{\theta})^{-1} \simeq \mathbf{CRLB}_{\mathrm{c}}(\boldsymbol{\theta}^{\mathrm{o}})^{-1}$, from which it can be further inferred that

$$\mathrm{cov}(\boldsymbol{\theta}) \simeq \mathbf{CRLB}_{\mathrm{c}}(\boldsymbol{\theta}^{\mathrm{o}}) \tag{84}$$

That is, the proposed solution accomplishes the CRLB accuracy if the two sets of conditions C1 and C2 are satisfied.

V. SIMULATION RESULTS

In this section, we proceed to assess the performance of the proposed solution via numerical simulations. Unless otherwise stated, we consider an MPR system with $M = 3$ transmitters, $N = 4$ receivers and $K = 5$ calibration targets, the positions and velocities of which are the same as those in TABLE 1. The localization accuracy is measured using root mean squares error (RMSE), which comes from 5000 independent Monte Carlo trials. In each trial, the zero-mean Gaussian random errors with covariance matrices $\mathbf{Q}_{\boldsymbol{\alpha}} = \mathrm{diag}\{\sigma_{\boldsymbol{\alpha}}^2\mathbf{I}_{MN}, 0.01\sigma_{\boldsymbol{\alpha}}^2\mathbf{I}_{MN}\}$, $\mathbf{Q}_{\boldsymbol{\beta}} = \mathrm{diag}\{\sigma_{\boldsymbol{\beta}}^2\mathbf{I}_{3(M+N)}, 0.01\sigma_{\boldsymbol{\beta}}^2\mathbf{I}_{3(M+N)}\}$, $\mathbf{Q}_{\boldsymbol{\gamma}} = \mathrm{diag}\{\sigma_{\boldsymbol{\gamma}}^2\mathbf{I}_{3K}, 0.01\sigma_{\boldsymbol{\gamma}}^2\mathbf{I}_{3K}\}$ and $\mathbf{Q}_{\boldsymbol{\alpha}\mathrm{c}} = \mathrm{diag}\{\sigma_{\boldsymbol{\alpha}}^2\mathbf{I}_{KMN}, 0.01\sigma_{\boldsymbol{\alpha}}^2\mathbf{I}_{KMN}\}$ are added to the BRs/BRRs from the unknown target, the actual transmitter/receiver locations, and the actual calibration target locations, and the BRs/BRRs from the calibration targets, respectively, in order to simulate a realistic localization scenario.

As mentioned in the Introduction part, Refs. [8], [9] and [10] investigate the moving target localization without considering the transmitter and receiver location uncertainties, and Ref. [15] considers the transmitter and receiver location error but does not use any calibration targets. In Refs. [10] and [15], theoretical analysis and simulation results have shown that the algorithm in Ref. [10] outperforms those proposed in Refs. [8] and [9]. Hence, for the sake of simplicity, comparison among the algorithms in Refs. [8], [9] and [10] will not be repeated. The interested reader is referred to [10] and [15] for details. In order to protrude the superiority of the proposed solution, the algorithm proposed in [10] which is regarded as the representative of the localization algorithms without considering the transmitter and receiver location errors, and that proposed in [15] which considers the statistical distributions of transmitter/receiver location error but does not use any calibration targets, are chosen as references for comparison.

As analyzed in Section IV-B, the localization accuracy of the proposed solution is related to the distance between the target and MPR system. Hence, in order to achieve a more comprehensive insight on the performance of the proposed solution, we consider two cases, i.e. near-field case where the target is close to the MPR system, and far-field case where the target is far away from the MPR system. We first address the far-field target, the position and velocity of which are set as $\mathbf{u}^{\mathrm{o}} = [180000, 18000, 18000]^{\mathrm{T}}$m and $\dot{\mathbf{u}}^{\mathrm{o}} = [500, 500, 50]^{\mathrm{T}}$ m/s respectively. The results are presented in FIGURE 4.

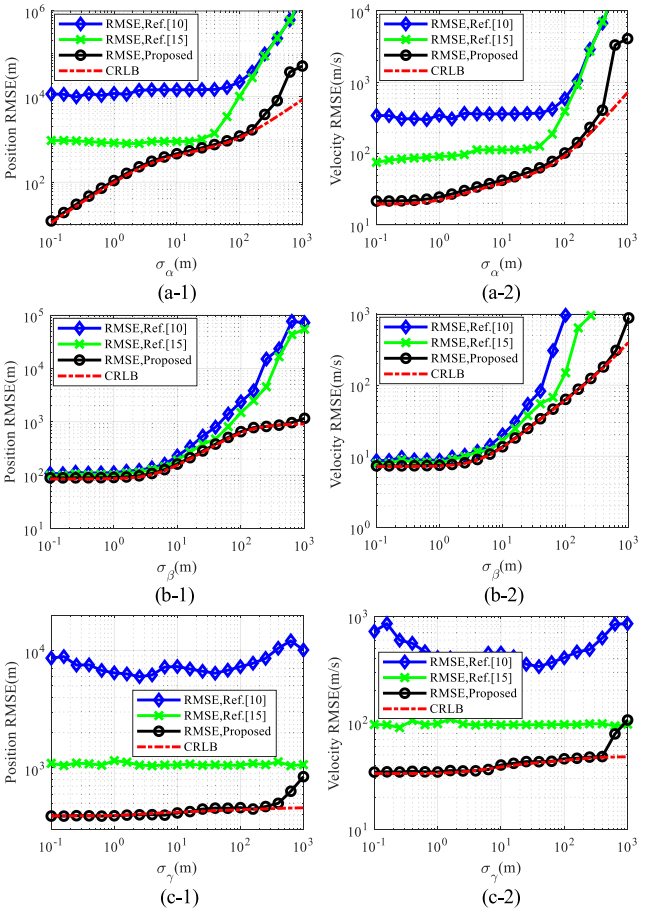

FIGURE 4. Comparison of the RMSEs among different localization algorithms in the far-field case: (a-1) position estimation accuracy as σ_α increases and $\sigma_\beta = 50$m, $\sigma_\gamma = 10$m; (a-2) velocity estimation accuracy as σ_α increases and $\sigma_\beta = 50$m, $\sigma_\gamma = 10$m; (b-1) position estimation accuracy as σ_β increases and $\sigma_\alpha = 10$m, $\sigma_\gamma = 10$m; (b-2) velocity estimation accuracy σ_β increases and $\sigma_\alpha = 10$m, $\sigma_\beta = 50$m.

FIGURE 4(a-1) and FIGURE 4(a-2) plot the position RMSE curves and velocity curves of the algorithms versus the BR/BRR measurement noise level. It shows that the localization RMSE of the proposed solution matches the CRLB very well and much lower than that of the algorithms in Refs. [10] and [15], at low to moderate BR/BRR measurement noise level. Although it deviates from the CRLB when the BR and BRR measurement noise is large, it is still much smaller than that of other two algorithms. And the deviation from the CRLB, known as thresholding phenomenon, is due to the ignored second order error terms in the design of the solution, which is invalid for large error levels. Owing to considering the statistical distributions of the transmitter/receiver location

error, the RMSEs produced by the algorithm in Ref. [15] is generally lower than that by the algorithm in Ref. [10]. But compared with the use of the calibration targets in the proposed solution, the localization accuracy improvement brought by the consideration of transmitter/receiver location uncertainties in Ref. [15] is not sufficiently impressive. FIGURE 4(b-1) and FIGURE 4(b-2) give the position RMSE curves and velocity curves of the algorithms versus the transmitter/receiver location uncertainty level. It can be seen that, the superiority of the proposed solution in localization accuracy is mainly reflected at moderate to high transmitter/receiver location uncertainty level. When the transmitter/receiver location error is small, the localization accuracy of the proposed solution and the other two algorithms is comparable. This again agrees very well with the theoretical performance in Section III. FIGURE 4(c-1) and FIGURE 4(c-2) compare the RMSEs from the algorithms with respect to different calibration target location error levels. As is illustrated in FIGURE 4(c-1) and FIGURE 4(c-2), the proposed solution always offers a remarkable advantage over the other two algorithms at low to moderate calibration target location error levels. At a calibration target location error level of $\sigma_{\boldsymbol{\gamma}} = 1000$m, the proposed solution deviates from the CRLB and loses its superiority over the algorithm in Ref. [15]. However, such a high calibration target location error is very rare in practice, since the calibration targets are well-chosen and cooperative.

Next, the same set of simulations was repeated for a near-field target, the position and velocity of which are set as $\mathbf{u}^{\mathrm{o}} = [18000, 1800, 1800]^{\mathrm{T}}$m and $\dot{\mathbf{u}}^{\mathrm{o}} = [500, 500, 50]^{\mathrm{T}}$m/s. The results are provided in FIGURE 5.

FIGURE 5 plots the comparison results in a near-field case. It can be seen from FIGURE 5 that the proposed solution still performs much better than the other algorithms. However, comparing with the corresponding results in FIGURE 4, we find the localization accuracy for near-field target is generally better than a far-field target, given the same measurement noise and transmitter/receiver/calibration target location error levels. One reason may be that, when the target is close to the MPR system, the transmitters/receivers are far apart relative to the distance between the target and the MPR system. Thus, the localization geometry would become more regular and the corresponding geometric dilution of precision (GDOP) value would be smaller compared to the far-field case. Nevertheless, on the other hand, comparing the thresholding values in FIGURE 5 and FIGURE 4 indicates that the RMSE curves for the near-field target deviate from the CRLB at smaller threshold values than those for the far-field target. This phenomenon is consistent with the analysis under conditions C1 and C2 that the equivalency between the estimate variance and the CRLB is more affected by the BR/BRR measurement noises when the target is close to the MPR system. It is also worth noting in FIGURE 5(b-1) and FIGURE 5(b-2) that at a transmitter/receiver location uncertainty level $\sigma_{\boldsymbol{\beta}} = 200$m, the RMSE of the proposed solution is even smaller than the CRLB. Similar phenomenon

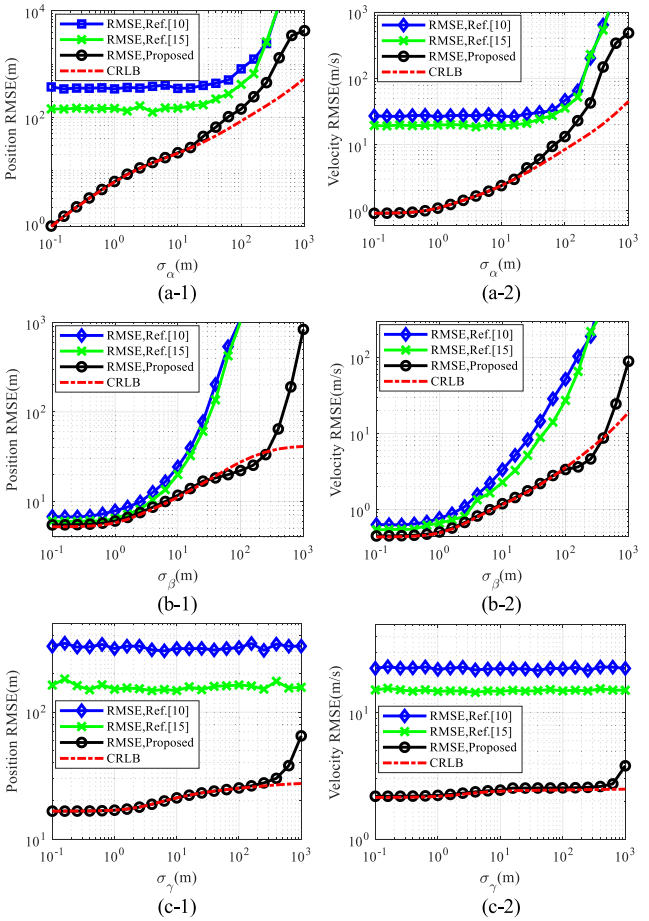

FIGURE 5. Comparison of the RMSEs among different localization algorithms in the far-field case: (a-1) position estimation accuracy as σ_α increases and $\sigma_\beta = 50$m, $\sigma_\gamma = 10$m; (a-2) velocity estimation accuracy as σ_α increases and $\sigma_\beta = 50$m, $\sigma_\gamma = 10$m; (b-1) position estimation accuracy as σ_β increases and $\sigma_\alpha = 10$m, $\sigma_\gamma = 10$m; (b-2) velocity estimation accuracy σ_β increases and $\sigma_\alpha = 10$m, $\sigma_\beta = 50$m.

has also been reported from previous studies on source localization problem [26]. A plausible explanation is that for this transmitter/receiver location uncertainty level, the second-order error terms cannot be ignored and the proposed solution would give a biased estimate. When an estimate is biased, its RMSE can be smaller than the CRLB [25]. In theory, if the two sets of conditions C1 and C2 are not satisfied, the proposed solution strictly speaking cannot be regarded as an unbiased estimate, and this phenomenon would potentially appear.

At an intuitive level, the more calibration targets are used, the better the localization accuracy is. In what follows, we will quantitatively analyze the effect of number of calibration targets on the localization accuracy by varying the number of calibration targets from 0 to 10. The positions and velocities of the transmitters and receivers remain the same as before. The location parameters of calibration targets and unknown target are chosen randomly from parameter space with lower bound [0km, −30km, 0km, −600m/s, −600m/s, −100m/s]$^{\mathrm{T}}$ and upper bound [60km, 30km, 60km, 600m/s,

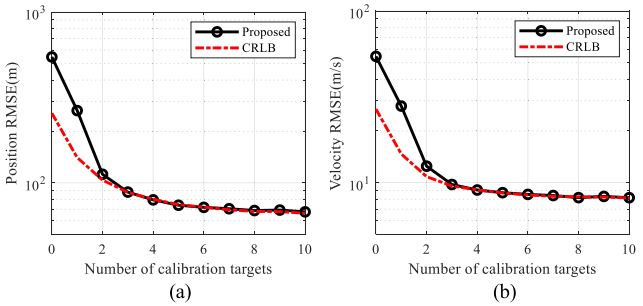

FIGURE 6. Localization accuracy versus the number of calibration targets.

600m/s, 100m/s]$^{\mathrm{T}}$. The simulation results are depicted in FIGURE 6.

FIGURE 6 shows the localization RMSE as well as the CRLB, versus the number of calibration targets. As expected, when the number of calibration targets is small, the localization accuracy improves significantly as the number of calibration targets increases. However, as soon as the number of calibration targets increases to more than 5, the improvement rate decreases radically. That is, by increasing the number of calibration targets, the localization RMSE with respect to the number of calibration targets tends to a bound.

VI. CONCLUSION

This paper explores the use of calibration targets with known positions and velocities to refine the inaccurate transmitter/receiver locations and thus enhance target localization accuracy in MPR system. We start our research by evaluating the target localization CRLB in the presence of calibration targets, which justifies the potential of calibration targets in enhancing localization accuracy. Then, in order to fulfill this potential, a novel closed-form solution was designed for target localization using BR and BRR measurements from the unknown target as well as those from the calibration targets. The proposed solution was shown both analytically and numerically to attain the CRLB under some mild conditions, and verified to outperform existing algorithms in terms of target localization accuracy. Furthermore, from the view of engineering practice, if the employed calibration targets are off-the-shelf, such as the commercial aircrafts broadcasting ADS-B signal, the use of calibration targets would bring little added cost or complexity to the MPR system, but could bring a significant enhancement to the target localization accuracy.

APPENDIX

First, we will derive the detailed expression of partial derivative $\partial\boldsymbol{\alpha}^{\mathrm{o}}/\partial\boldsymbol{\theta}^{\mathrm{o}}$. Considering the structure of $\partial\boldsymbol{\alpha}^{\mathrm{o}}/\partial\boldsymbol{\theta}^{\mathrm{o}}$ has to do with the order of the elements arranged in $\boldsymbol{\alpha}^{\mathrm{o}}$ and $\boldsymbol{\theta}^{\mathrm{o}}$, it is natural to divide it into four block submatrices as

$$\frac{\partial\boldsymbol{\alpha}^{\mathrm{o}}}{\partial\boldsymbol{\theta}^{\mathrm{o}}}=\begin{bmatrix}\dfrac{\partial\mathbf{r}^{\mathrm{o}}}{\partial\mathbf{u}^{\mathrm{o}}} & \dfrac{\partial\mathbf{r}^{\mathrm{o}}}{\partial\dot{\mathbf{u}}^{\mathrm{o}}}\\ \dfrac{\partial\dot{\mathbf{r}}^{\mathrm{o}}}{\partial\mathbf{u}^{\mathrm{o}}} & \dfrac{\partial\dot{\mathbf{r}}^{\mathrm{o}}}{\partial\dot{\mathbf{u}}^{\mathrm{o}}}\end{bmatrix} \tag{85}$$

According to (8) and (9), the elements of block submatrices $\partial\mathbf{r}^{\mathrm{o}}/\partial\mathbf{u}^{\mathrm{o}}$, $\partial\mathbf{r}^{\mathrm{o}}/\partial\dot{\mathbf{u}}^{\mathrm{o}}$, $\partial\dot{\mathbf{r}}^{\mathrm{o}}/\partial\mathbf{u}^{\mathrm{o}}$ and $\partial\dot{\mathbf{r}}^{\mathrm{o}}/\partial\dot{\mathbf{u}}^{\mathrm{o}}$ are further given by

$$\left[\frac{\partial\mathbf{r}^{\mathrm{o}}}{\partial\mathbf{u}^{\mathrm{o}}}\right]_{(m-1)N+n,1:3}=\frac{(\mathbf{u}^{\mathrm{o}}-\mathbf{s}_{\mathrm{t},m}^{\mathrm{o}})^{\mathrm{T}}}{R_{\mathrm{t},m}^{\mathrm{o}}}+\frac{(\mathbf{u}^{\mathrm{o}}-\mathbf{s}_{\mathrm{r},n}^{\mathrm{o}})^{\mathrm{T}}}{R_{\mathrm{r},n}^{\mathrm{o}}}$$

$$\left[\frac{\partial\mathbf{r}^{\mathrm{o}}}{\partial\dot{\mathbf{u}}^{\mathrm{o}}}\right]_{(m-1)N+n,1:3}=\mathbf{0}_{3\times1}^{\mathrm{T}}$$

$$\left[\frac{\partial\dot{\mathbf{r}}^{\mathrm{o}}}{\partial\mathbf{u}^{\mathrm{o}}}\right]_{(m-1)N+n,1:3}=\frac{(\dot{\mathbf{u}}^{\mathrm{o}}-\dot{\mathbf{s}}_{\mathrm{t},m}^{\mathrm{o}})^{\mathrm{T}}R_{\mathrm{t},m}^{\mathrm{o}}-(\mathbf{u}^{\mathrm{o}}-\mathbf{s}_{\mathrm{t},m}^{\mathrm{o}})^{\mathrm{T}}\dot{R}_{\mathrm{t},m}^{\mathrm{o}}}{(R_{\mathrm{t},m}^{\mathrm{o}})^{2}}+\frac{(\dot{\mathbf{u}}^{\mathrm{o}}-\dot{\mathbf{s}}_{\mathrm{r},n}^{\mathrm{o}})^{\mathrm{T}}R_{\mathrm{r},n}^{\mathrm{o}}-(\mathbf{u}^{\mathrm{o}}-\mathbf{s}_{\mathrm{r},n}^{\mathrm{o}})^{\mathrm{T}}\dot{R}_{\mathrm{r},n}^{\mathrm{o}}}{(R_{\mathrm{r},n}^{\mathrm{o}})^{2}}$$

$$\left[\frac{\partial\dot{\mathbf{r}}^{\mathrm{o}}}{\partial\dot{\mathbf{u}}^{\mathrm{o}}}\right]_{(m-1)N+n,1:3}=\frac{(\mathbf{u}^{\mathrm{o}}-\mathbf{s}_{\mathrm{t},m}^{\mathrm{o}})^{\mathrm{T}}}{R_{\mathrm{t},m}^{\mathrm{o}}}+\frac{(\mathbf{u}^{\mathrm{o}}-\mathbf{s}_{\mathrm{r},n}^{\mathrm{o}})^{\mathrm{T}}}{R_{\mathrm{r},n}^{\mathrm{o}}}$$

for $m=1,2,\ldots,M$, $n=1,2,\ldots,N$.

In like manner, the partial derivative $\partial\boldsymbol{\alpha}^{\mathrm{o}}/\partial\boldsymbol{\beta}^{\mathrm{o}}$ can be partitioned as

$$\frac{\partial\boldsymbol{\alpha}^{\mathrm{o}}}{\partial\boldsymbol{\beta}^{\mathrm{o}}}=\begin{bmatrix}\dfrac{\partial\mathbf{r}^{\mathrm{o}}}{\partial\mathbf{s}_{\mathrm{t}}^{\mathrm{o}}} & \dfrac{\partial\mathbf{r}^{\mathrm{o}}}{\partial\mathbf{s}_{\mathrm{r}}^{\mathrm{o}}} & \dfrac{\partial\mathbf{r}^{\mathrm{o}}}{\partial\dot{\mathbf{s}}_{\mathrm{t}}^{\mathrm{o}}} & \dfrac{\partial\mathbf{r}^{\mathrm{o}}}{\partial\dot{\mathbf{s}}_{\mathrm{r}}^{\mathrm{o}}}\\ \dfrac{\partial\dot{\mathbf{r}}^{\mathrm{o}}}{\partial\mathbf{s}_{\mathrm{t}}^{\mathrm{o}}} & \dfrac{\partial\dot{\mathbf{r}}^{\mathrm{o}}}{\partial\mathbf{s}_{\mathrm{r}}^{\mathrm{o}}} & \dfrac{\partial\dot{\mathbf{r}}^{\mathrm{o}}}{\partial\dot{\mathbf{s}}_{\mathrm{t}}^{\mathrm{o}}} & \dfrac{\partial\dot{\mathbf{r}}^{\mathrm{o}}}{\partial\dot{\mathbf{s}}_{\mathrm{r}}^{\mathrm{o}}}\end{bmatrix} \tag{86}$$

and the elements of the involved submatrices are given by

$$\left[\frac{\partial\mathbf{r}^{\mathrm{o}}}{\partial\mathbf{s}_{\mathrm{t}}^{\mathrm{o}}}\right]_{(m-1)N+n,3m-2:3m}=\frac{(\mathbf{s}_{\mathrm{t},m}^{\mathrm{o}}-\mathbf{u}^{\mathrm{o}})^{\mathrm{T}}}{R_{\mathrm{t},m}^{\mathrm{o}}}$$

$$\left[\frac{\partial\mathbf{r}^{\mathrm{o}}}{\partial\mathbf{s}_{\mathrm{r}}^{\mathrm{o}}}\right]_{(m-1)N+n,3n-2:3n}=\frac{(\mathbf{s}_{\mathrm{r},n}^{\mathrm{o}}-\mathbf{u}^{\mathrm{o}})^{\mathrm{T}}}{R_{\mathrm{r},n}^{\mathrm{o}}}$$

$$\left[\frac{\partial\mathbf{r}^{\mathrm{o}}}{\partial\dot{\mathbf{s}}_{\mathrm{t}}^{\mathrm{o}}}\right]_{(m-1)N+n,3m-2:3m}=\mathbf{0}_{3\times1}^{\mathrm{T}}$$

$$\left[\frac{\partial\mathbf{r}^{\mathrm{o}}}{\partial\dot{\mathbf{s}}_{\mathrm{r}}^{\mathrm{o}}}\right]_{(m-1)N+n,3n-2:3n}=\mathbf{0}_{3\times1}^{\mathrm{T}}$$

$$\left[\frac{\partial\dot{\mathbf{r}}^{\mathrm{o}}}{\partial\mathbf{s}_{\mathrm{t}}^{\mathrm{o}}}\right]_{(m-1)N+n,3m-2:3m}=\frac{(\dot{\mathbf{s}}_{\mathrm{t},m}^{\mathrm{o}}-\dot{\mathbf{u}}^{\mathrm{o}})^{\mathrm{T}}R_{\mathrm{t},m}^{\mathrm{o}}-(\mathbf{s}_{\mathrm{t},m}^{\mathrm{o}}-\mathbf{u}^{\mathrm{o}})^{\mathrm{T}}\dot{R}_{\mathrm{t},m}^{\mathrm{o}}}{(R_{\mathrm{t},m}^{\mathrm{o}})^{2}}$$

$$\left[\frac{\partial\dot{\mathbf{r}}^{\mathrm{o}}}{\partial\mathbf{s}_{\mathrm{r}}^{\mathrm{o}}}\right]_{(m-1)N+n,3n-2:3n}=\frac{(\dot{\mathbf{s}}_{\mathrm{r},n}^{\mathrm{o}}-\dot{\mathbf{u}}^{\mathrm{o}})^{\mathrm{T}}R_{\mathrm{r},n}^{\mathrm{o}}-(\mathbf{s}_{\mathrm{r},n}^{\mathrm{o}}-\mathbf{u}^{\mathrm{o}})^{\mathrm{T}}\dot{R}_{\mathrm{r},n}^{\mathrm{o}}}{(R_{\mathrm{r},n}^{\mathrm{o}})^{2}}$$

$$\left[\frac{\partial\dot{\mathbf{r}}^{\mathrm{o}}}{\partial\dot{\mathbf{s}}_{\mathrm{t}}^{\mathrm{o}}}\right]_{(m-1)N+n,3m-2:3m}=\frac{(\mathbf{s}_{\mathrm{t},m}^{\mathrm{o}}-\mathbf{u}^{\mathrm{o}})^{\mathrm{T}}}{R_{\mathrm{t},m}^{\mathrm{o}}}$$

$$\left[\frac{\partial\dot{\mathbf{r}}^{\mathrm{o}}}{\partial\dot{\mathbf{s}}_{\mathrm{r}}^{\mathrm{o}}}\right]_{(m-1)N+n,3n-2:3n}=\frac{(\mathbf{s}_{\mathrm{r},n}^{\mathrm{o}}-\mathbf{u}^{\mathrm{o}})^{\mathrm{T}}}{R_{\mathrm{r},n}^{\mathrm{o}}}$$

for $m=1,2,\ldots,M$, $n=1,2,\ldots,N$.

The partial derivative $\partial\boldsymbol{\alpha}_{\mathrm{c}}^{\mathrm{o}}/\partial\boldsymbol{\beta}^{\mathrm{o}}$ can be written as

$$\frac{\partial\boldsymbol{\alpha}_{\mathrm{c}}^{\mathrm{o}}}{\partial\boldsymbol{\beta}^{\mathrm{o}}}=\begin{bmatrix}\dfrac{\partial\mathbf{r}_{\mathrm{c}}^{\mathrm{o}}}{\partial\mathbf{s}_{\mathrm{t}}^{\mathrm{o}}} & \dfrac{\partial\mathbf{r}_{\mathrm{c}}^{\mathrm{o}}}{\partial\mathbf{s}_{\mathrm{r}}^{\mathrm{o}}} & \dfrac{\partial\mathbf{r}_{\mathrm{c}}^{\mathrm{o}}}{\partial\dot{\mathbf{s}}_{\mathrm{t}}^{\mathrm{o}}} & \dfrac{\partial\mathbf{r}_{\mathrm{c}}^{\mathrm{o}}}{\partial\dot{\mathbf{s}}_{\mathrm{r}}^{\mathrm{o}}}\\ \dfrac{\partial\dot{\mathbf{r}}_{\mathrm{c}}^{\mathrm{o}}}{\partial\mathbf{s}_{\mathrm{t}}^{\mathrm{o}}} & \dfrac{\partial\dot{\mathbf{r}}_{\mathrm{c}}^{\mathrm{o}}}{\partial\mathbf{s}_{\mathrm{r}}^{\mathrm{o}}} & \dfrac{\partial\dot{\mathbf{r}}_{\mathrm{c}}^{\mathrm{o}}}{\partial\dot{\mathbf{s}}_{\mathrm{t}}^{\mathrm{o}}} & \dfrac{\partial\dot{\mathbf{r}}_{\mathrm{c}}^{\mathrm{o}}}{\partial\dot{\mathbf{s}}_{\mathrm{r}}^{\mathrm{o}}}\end{bmatrix} \tag{87}$$

with the elements of the involved submatrices given by

$$\left[\frac{\partial \mathbf{r}_{\mathrm{c}}^{\mathrm{o}}}{\partial \mathbf{s}_{\mathrm{t}}^{\mathrm{o}}}\right]_{(k-1)MN+(m-1)N+n,3m-2:3m} = \frac{(\mathbf{s}_{\mathrm{t},m}^{\mathrm{o}}-\mathbf{c}_k^{\mathrm{o}})^{\mathrm{T}}}{R_{\mathrm{c},k,\mathrm{t},m}^{\mathrm{o}}}$$

$$\left[\frac{\partial \mathbf{r}_{\mathrm{c}}^{\mathrm{o}}}{\partial \mathbf{s}_{\mathrm{t}}^{\mathrm{o}}}\right]_{(k-1)MN+(m-1)N+n,3n-2:3n} = \frac{(\mathbf{s}_{\mathrm{r},n}^{\mathrm{o}}-\mathbf{c}_k^{\mathrm{o}})^{\mathrm{T}}}{R_{\mathrm{c},k,\mathrm{r},n}^{\mathrm{o}}}$$

$$\left[\frac{\partial \mathbf{r}_{\mathrm{c}}^{\mathrm{o}}}{\partial \dot{\mathbf{s}}_{\mathrm{t}}^{\mathrm{o}}}\right]_{(k-1)MN+(m-1)N+n,3m-2:3m} = \mathbf{0}_{3\times 1}^{\mathrm{T}}$$

$$\left[\frac{\partial \mathbf{r}_{\mathrm{c}}^{\mathrm{o}}}{\partial \dot{\mathbf{s}}_{\mathrm{r}}^{\mathrm{o}}}\right]_{(k-1)MN+(m-1)N+n,3n-2:3n} = \mathbf{0}_{3\times 1}^{\mathrm{T}}$$

$$\left[\frac{\partial \dot{\mathbf{r}}_{\mathrm{c}}^{\mathrm{o}}}{\partial \mathbf{s}_{\mathrm{t}}^{\mathrm{o}}}\right]_{(k-1)MN+(m-1)N+n,3m-2:3m} = \frac{(\dot{\mathbf{s}}_{\mathrm{t},m}^{\mathrm{o}}-\dot{\mathbf{c}}_k^{\mathrm{o}})^{\mathrm{T}}}{R_{\mathrm{c},k,\mathrm{t},m}^{\mathrm{o}}} - \frac{(\mathbf{s}_{\mathrm{t},m}^{\mathrm{o}}-\mathbf{c}_k^{\mathrm{o}})^{\mathrm{T}}\dot{R}_{\mathrm{c},k,\mathrm{t},m}^{\mathrm{o}}}{(R_{\mathrm{c},k,\mathrm{t},m}^{\mathrm{o}})^2}$$

$$\left[\frac{\partial \dot{\mathbf{r}}_{\mathrm{c}}^{\mathrm{o}}}{\partial \mathbf{s}_{\mathrm{r}}^{\mathrm{o}}}\right]_{(k-1)MN+(m-1)N+n,3n-2:3n} = \frac{(\dot{\mathbf{s}}_{\mathrm{r},n}^{\mathrm{o}}-\dot{\mathbf{c}}_k^{\mathrm{o}})^{\mathrm{T}}}{R_{\mathrm{c},k,\mathrm{r},n}^{\mathrm{o}}} - \frac{(\mathbf{s}_{\mathrm{r},n}^{\mathrm{o}}-\mathbf{c}_k^{\mathrm{o}})^{\mathrm{T}}\dot{R}_{\mathrm{c},k,\mathrm{r},n}^{\mathrm{o}}}{(R_{\mathrm{c},k,\mathrm{r},n}^{\mathrm{o}})^2}$$

$$\left[\frac{\partial \dot{\mathbf{r}}_{\mathrm{c}}^{\mathrm{o}}}{\partial \dot{\mathbf{s}}_{\mathrm{t}}^{\mathrm{o}}}\right]_{(k-1)MN+(m-1)N+n,3m-2:3m} = \frac{(\mathbf{s}_{\mathrm{t},m}^{\mathrm{o}}-\mathbf{c}_k^{\mathrm{o}})^{\mathrm{T}}}{R_{\mathrm{c},k,\mathrm{t},m}^{\mathrm{o}}}$$

$$\left[\frac{\partial \dot{\mathbf{r}}_{\mathrm{c}}^{\mathrm{o}}}{\partial \dot{\mathbf{s}}_{\mathrm{r}}^{\mathrm{o}}}\right]_{(k-1)MN+(m-1)N+n,3n-2:3n} = \frac{(\mathbf{s}_{\mathrm{r},n}^{\mathrm{o}}-\mathbf{c}_k^{\mathrm{o}})^{\mathrm{T}}}{R_{\mathrm{c},k,\mathrm{r},n}^{\mathrm{o}}}$$

for $k = 1, 2, \ldots, K$, $m = 1, 2, \ldots, M$, $n = 1, 2, \ldots, N$.

The partial derivative $\partial \boldsymbol{\alpha}_{\mathrm{c}}^{\mathrm{o}} / \partial \boldsymbol{\gamma}^{\mathrm{o}}$ can be given as

$$\frac{\partial \boldsymbol{\alpha}_{\mathrm{c}}^{\mathrm{o}}}{\partial \boldsymbol{\gamma}^{\mathrm{o}}} = \begin{bmatrix} \dfrac{\partial \mathbf{r}_{\mathrm{c}}^{\mathrm{o}}}{\partial \mathbf{c}^{\mathrm{o}}} & \dfrac{\partial \mathbf{r}_{\mathrm{c}}^{\mathrm{o}}}{\partial \dot{\mathbf{c}}^{\mathrm{o}}} \\ \dfrac{\partial \dot{\mathbf{r}}_{\mathrm{c}}^{\mathrm{o}}}{\partial \mathbf{c}^{\mathrm{o}}} & \dfrac{\partial \dot{\mathbf{r}}_{\mathrm{c}}^{\mathrm{o}}}{\partial \dot{\mathbf{c}}^{\mathrm{o}}} \end{bmatrix} \tag{88}$$

with the elements of the involved submatrices given by

$$\left[\frac{\partial \mathbf{r}_{\mathrm{c}}^{\mathrm{o}}}{\partial \mathbf{c}^{\mathrm{o}}}\right]_{(k-1)MN+(m-1)N+n,3k-2:3k} = \frac{(\mathbf{c}_k^{\mathrm{o}}-\mathbf{s}_{\mathrm{t},m}^{\mathrm{o}})^{\mathrm{T}}}{R_{\mathrm{c},k,\mathrm{t},m}^{\mathrm{o}}} + \frac{(\mathbf{c}_k^{\mathrm{o}}-\mathbf{s}_{\mathrm{r},n}^{\mathrm{o}})^{\mathrm{T}}}{R_{\mathrm{c},k,\mathrm{r},n}^{\mathrm{o}}}$$

$$\left[\frac{\partial \mathbf{r}_{\mathrm{c}}^{\mathrm{o}}}{\partial \dot{\mathbf{c}}^{\mathrm{o}}}\right]_{(k-1)MN+(m-1)N+n,3k-2:3k} = \mathbf{0}_{3\times 1}^{\mathrm{T}}$$

$$\left[\frac{\partial \dot{\mathbf{r}}_{\mathrm{c}}^{\mathrm{o}}}{\partial \mathbf{c}^{\mathrm{o}}}\right]_{(k-1)MN+(m-1)N+n,3k-2:3k} = \frac{(\dot{\mathbf{c}}_k^{\mathrm{o}}-\dot{\mathbf{s}}_{\mathrm{t},m}^{\mathrm{o}})^{\mathrm{T}}}{R_{\mathrm{c},k,\mathrm{t},m}^{\mathrm{o}}} - \frac{(\mathbf{c}_k^{\mathrm{o}}-\mathbf{s}_{\mathrm{t},m}^{\mathrm{o}})^{\mathrm{T}}\dot{R}_{\mathrm{c},k,\mathrm{t},m}^{\mathrm{o}}}{(R_{\mathrm{c},k,\mathrm{t},m}^{\mathrm{o}})^2} + \frac{(\dot{\mathbf{c}}_k^{\mathrm{o}}-\dot{\mathbf{s}}_{\mathrm{r},n}^{\mathrm{o}})^{\mathrm{T}}}{R_{\mathrm{c},k,\mathrm{r},n}^{\mathrm{o}}} - \frac{(\mathbf{c}_k^{\mathrm{o}}-\mathbf{s}_{\mathrm{r},n}^{\mathrm{o}})^{\mathrm{T}}\dot{R}_{\mathrm{c},k,\mathrm{r},n}^{\mathrm{o}}}{(R_{\mathrm{c},k,\mathrm{r},n}^{\mathrm{o}})^2}$$

$$\left[\frac{\partial \dot{\mathbf{r}}_{\mathrm{c}}^{\mathrm{o}}}{\partial \dot{\mathbf{c}}^{\mathrm{o}}}\right]_{(k-1)MN+(m-1)N+n,3k-2:3k} = \frac{(\mathbf{c}_k^{\mathrm{o}}-\mathbf{s}_{\mathrm{t},m}^{\mathrm{o}})^{\mathrm{T}}}{R_{\mathrm{c},k,\mathrm{t},m}^{\mathrm{o}}} + \frac{(\mathbf{c}_k^{\mathrm{o}}-\mathbf{s}_{\mathrm{r},n}^{\mathrm{o}})^{\mathrm{T}}}{R_{\mathrm{c},k,\mathrm{r},n}^{\mathrm{o}}}$$

for $k = 1, 2, \ldots, K$, $m = 1, 2, \ldots, M$, $n = 1, 2, \ldots, N$.

REFERENCES

[1] J. Palmer, S. Palumbo, A. Summers, D. Merrett, S. Searle, and S. Howard, "An overview of an illuminator of opportunity passive radar research project and its signal processing research directions," *Digit. Signal Process.*, vol. 21, no. 5, pp. 593–599, Sep. 2011.
[2] Y. Wang, Q. Bao, D. Wang, and Z. Chen, "An experimental study of passive bistatic radar using uncooperative radar as a transmitter," *IEEE Geosci. Remote Sens. Lett.*, vol. 12, no. 9, pp. 1868–1872, Sep. 2015.
[3] K. E. Olsen and W. Asen, "Bridging the gap between civilian and military passive radar," *IEEE Aerosp. Electron. Syst. Mag.*, vol. 32, no. 2, pp. 4–12, Feb. 2017.
[4] M. Edrich, A. Schroeder, and F. Meyer, "Design and performance evaluation of a mature FM/DAB/DVB-T multi-illuminator passive radar system," *IET Radar, Sonar Navigat.*, vol. 8, no. 2, pp. 114–122, Feb. 2014.
[5] X. Zhang, H. Li, J. Liu, and B. Himed, "Joint delay and Doppler estimation for passive sensing with direct-path interference," *IEEE Trans. Signal Process.*, vol. 64, no. 3, pp. 630–640, Feb. 2016.
[6] M. Malanowski and K. Kulpa, "Two methods for target localization in multistatic passive radar," *IEEE Trans. Aerosp. Electron. Syst.*, vol. 48, no. 1, pp. 572–580, Jan. 2012.
[7] K. C. Ho and W. Xu, "An accurate algebraic solution for moving source location using TDOA and FDOA measurements," *IEEE Trans. Signal Process.*, vol. 52, no. 9, pp. 2453–2463, Sep. 2004.
[8] Y. Du and P. Wei, "An explicit solution for target localization in noncoherent distributed MIMO radar systems," *IEEE Signal Process. Lett.*, vol. 21, no. 9, pp. 1093–1097, Sep. 2014.
[9] H. Yang and J. Chun, "An improved algebraic solution for moving target localization in noncoherent MIMO radar systems," *IEEE Trans. Signal Process.*, vol. 64, no. 1, pp. 258–270, Jan. 2015.
[10] Y. Zhao, Z. Yongjun, and C. Zhao, "A novel algebraic solution for moving target localization in multi-transmitter multi-receiver passive radar," *Signal Process.*, vol. 143, pp. 303–310, Feb. 2018.
[11] B. Dawidowicz, K. S. Kulpa, M. Malanowski, J. Misiurewicz, P. Samczynski, and M. Smolarczyk, "DPCA detection of moving targets in airborne passive radar," *IEEE Trans. Aerosp. Electron. Syst.*, vol. 48, no. 2, pp. 1347–1357, Apr. 2012.
[12] J. Brown, K. Woodbridge, H. Griffiths, A. Stove, and S. Watts, "Passive bistatic radar experiments from an airborne platform," *IEEE Aerosp. Electron. Syst. Mag.*, vol. 27, no. 11, pp. 50–55, Nov. 2012.
[13] E. C. Thompson, "Bistatic radar noncooperative illumination synchronization techniques," in *Proc. IEEE Nat. Radar Conf.*, Dallas, TX, USA, Mar. 1989, pp. 29–34.
[14] D. Matthes, "Convergence of ESM sensors and passive covert radar," in *Proc. IEEE Int. Radar Conf.*, Arlington, VA, USA, May 2005, pp. 430–444.
[15] Y. Zhao, D. Hu, Y. Zhao, and Z. Liu, "Moving target localization in distributed MIMO radar with transmitter and receiver location uncertainties," *Chin. J. Aeronaut.*, vol. 32, no. 7, pp. 1705–1715, Jul. 2019.
[16] R. Moses and R. Patterson, "Self-calibration of sensor networks," *Proc. SPIE*, vol. 4743, pp. 108–119, Aug. 2002.
[17] J. N. Ash and R. L. Moses, "On the relative and absolute positioning errors in self-localization systems," *IEEE Trans. Signal Process.*, vol. 56, no. 11, pp. 5668–5679, Nov. 2008.
[18] H. S. Mir, J. D. Sahr, G. F. Hatke, and C. M. Keller, "Passive source localization using an airborne sensor array in the presence of manifold perturbations," *IEEE Trans. Signal Process.*, vol. 55, no. 6, pp. 2486–2496, Jun. 2007.
[19] K. C. Ho and L. Yang, "On the use of a calibration emitter for source localization in the presence of sensor position uncertainty," *IEEE Trans. Signal Process.*, vol. 56, no. 12, pp. 5758–5772, Dec. 2008.
[20] L. Yang and K. C. Ho, "Alleviating sensor position error in source localization using calibration emitters at inaccurate locations," *IEEE Trans. Signal Process.*, vol. 58, no. 1, pp. 67–83, Jan. 2010.

[21] J. Li, F. Guo, L. Yang, W. Jiang, and H. Pang, "On the use of calibration sensors in source localization using TDOA and FDOA measurements," *Digit. Signal Process.*, vol. 27, pp. 33–43, Apr. 2014.
[22] M. Strohmeier, M. Schafer, V. Lenders, and I. Martinovic, "Realities and challenges of NextGen air traffic management: The case of ADS-B," *IEEE Commun. Mag.*, vol. 52, no. 5, pp. 111–118, May 2014.
[23] K. B. Petersen and M. S. Pedersen, "The matrix cookbook," Tech. Univ. Denmark, Kongens Lyngby, Denmark, Tech. Rep., 2012.
[24] R. Bellman, *Introduction to Matrix Analysis*. NewYork, NY, USA: McGraw-Hill, 1960.
[25] S. M. Kay, *Fundamentals of Statistical Signal Processing, Volume I: Estimation Theory*. Englewood Cliffs, NJ, USA: Prentice-Hall, 1993.
[26] L. Lin, H. C. So, F. K. W. Chan, Y. T. Chan, and K. C. Ho, "A new constrained weighted least squares algorithm for TDOA-based localization," *Signal Process.*, vol. 93, no. 11, pp. 2872–2878, 2013.

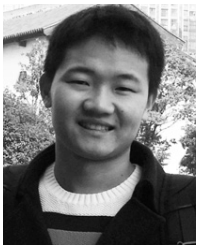

YONGSHENG ZHAO was born in Donghai, Lianyungang, Jiangsu, China, in 1990. He received the B.S. degree in electronic engineering from the Zhengzhou Information Science Technology Institute, Zhengzhou, China, in 2013, and the M.S. degree in information and communication engineering from the National Digital Switching System Engineering and Technological Research Center (NDSC), Zhengzhou, in 2016. He is currently pursuing the Ph.D. degree in information and communication engineering with PLA Strategic Support Force Information Engineering University, Zhengzhou. His current research interests include multistatic passive radar, target localization, radar signal processing, estimation theory, and detection theory.

DEXIU HU was born in China. He received the B.S. and M.S. degrees from the Zhengzhou Information Technology Institute, Zhengzhou, China, in 2007 and 2010, respectively, and the Ph.D. degree in electronic engineering from Tsinghua University, Beijing, China.

Since 2009, he has been a Lecturer with PLA Strategic Support Force Information Engineering University. He is the author of three books and more than 20 articles. His research interests include DOA estimation, passive location, and satellite communication.

ZHIXIN LIU was born in Urumchi, Xinjiang, China. He received the B.S. degree in electronic engineering from the Zhengzhou Information Technology Institute, Zhengzhou, China, in 2014, and the M.S. degree in information and communication engineering from the National Digital Switching System Engineering and Technological Research Center (NDSC), Zhengzhou, in 2017. He is currently pursuing the Ph.D. degree in information and communication engineering with PLA Strategic Support Force Information Engineering University, Zhengzhou. His current research interests include target detection, source localization, and estimation theory.

YONGJUN ZHAO was born in China. He received the B.S. and M.S. degrees from the Beijing Institute of Technology, Beijing, China, in 1985 and 2008, respectively.

He is currently a Professor with PLA Strategic Support Force Information Engineering University, Zhengzhou, China. He is the author of four books and more than 40 articles. He holds more than ten patents for inventions. His current research interests include radar signal processing and array signal processing.